JOHN WILEY & SONS, LTD., THE ATRIUM, SOUTHERN GATE, CHICHESTER P019 8SQ, UK

*****PROOF OF YOUR ARTICLE ATTACHED, PLEASE READ CAREFULLY*****

After receipt of your corrections your article will be published initially within the online version of the journal.

PLEASE AIM TO RETURN YOUR CORRECTIONS WITHIN 48 HOURS OF RECEIPT OF YOUR PROOF, THIS WILL ENSURE THAT THERE ARE NO UNNECESSARY DELAYS IN THE PUBLICATION OF YOUR ARTICLE

- **READ PROOFS CAREFULLY**

ONCE PUBLISHED ONLINE OR IN PRINT IT IS NOT POSSIBLE TO MAKE ANY FURTHER CORRECTIONS TO YOUR ARTICLE

  - This will be your only chance to correct your proof
  - Please note that the volume and page numbers shown on the proofs are for position only

- **ANSWER ALL QUERIES ON PROOFS** (Queries are attached as the last page of your proof.)

  - Please annotate this file electronically and return by email to the production contact as detailed in the covering email. Guidelines on using the electronic annotation tools can be found at the end of the proof. If you are unable to correct your proof using electronic annotation, please list all corrections and send back via email to the address in the covering email, or mark all corrections directly on the proofs and send the scanned copy via email. Please do not send corrections by fax or post.

  Acrobat Reader & Acrobat Professional
  - You will only be able to annotate the file using Acrobat Reader 8.0 or above and Acrobat Professional. Acrobat Reader can be downloaded free of charge at the following address: http://www.adobe.com/products/acrobat/readstep2.html

- **CHECK FIGURES AND TABLES CAREFULLY**

  - Check size, numbering, and orientation of figures
  - All images in the PDF are downsampled (reduced to lower resolution and file size) to facilitate Internet delivery. These images will appear at higher resolution and sharpness in the printed article
  - Review figure legends to ensure that they are complete
  - Check all tables. Review layout, title, and footnotes

- **COMPLETE COPYRIGHT TRANSFER AGREEMENT (CTA) if you have not already signed one**

  - Please send a scanned signed copy with your proofs by e-mail. **Your article cannot be published unless we have received the signed CTA**

- **OFFPRINTS**

  - Free access to the final PDF offprint or your article will be available via Author Services only. Please therefore sign up for Author Services if you would like to access your article PDF offprint and enjoy the many other benefits the service offers.

Additional reprint and journal issue purchases

  - Should you wish to purchase additional copies of your article, please click on the link and follow the instructions provided: http://offprint.cosprinters.com/cos/bw/
  - Corresponding authors are invited to inform their co-authors of the reprint options available.
  - Please note that regardless of the form in which they are acquired, reprints should not be resold, nor further disseminated in electronic form, nor deployed in part or in whole in any marketing, promotional or educational contexts without authorization from Wiley. Permissions requests should be directed to mailto: permissionsuk@wiley.com

HYDROLOGICAL PROCESSES
Hydrol. Process. **24**, 0–0 (2010)
Published online in Wiley Online Library
(wileyonlinelibrary.com) DOI: 10.1002/hyp.7926

Large-scale modelling of channel flow and floodplain inundation dynamics and its application to the Pantanal (Brazil)

Adriano Rolim da Paz,[1,2]* Walter Collischonn,[1] Carlos E. M. Tucci[1] and Carlos R. Padovani[3]

[1] *Instituto de Pesquisas Hidráulicas, Universidade Federal do Rio Grande do Sul, Av. Bento Gonçalves 9500, Agronomia, CEP 91501-970, Porto Alegre-RS, Brazil*
[2] *EMBRAPA Monitoramento por Satélite, Av. Soldado Passarinho 303, Fazenda Chapadão, CEP 13070-115, Campinas-SP, Brazil*
[3] *EMBRAPA Pantanal, Rua 21 de Setembro, 1880, Bairro Nossa Senhora de Fátima, CEP 79320-900, Corumbá-MS, Brazil*

Abstract:

For large-scale sites, difficulties for applying coupled one-dimensional (1D)/2D models for simulating floodplain inundation may be encountered related to data scarcity, complexity for establishing channel–floodplain connections, computational cost, long duration of floods and the need to represent precipitation and evapotranspiration processes. This paper presents a hydrologic simulation system, named SIRIPLAN, developed to accomplish this aim. This system is composed by a 1D hydrodynamic model coupled to a 2D raster-based model, and by two modules to compute the vertical water balance over floodplain and the water exchanges between channel and floodplain. Results are presented for the Upper Paraguay River Basin (UPRB), including the Pantanal, one of the world's largest wetlands. A total of 3965 km of river channels and 140 000 km^2 of floodplains are simulated for a period of 11 years. Comparison of observed and calculated hydrographs at 15 gauging stations showed that the model was capable to simulate distinct, complex flow regimes along main channels, including channel-floodplain interactions. The proposed system was also able to reproduce the Pantanal seasonal flood pulse, with estimated inundated areas ranging from 35 000 km^2 (dry period) to more than 120 000 km^2 (wet period). Floodplain inundation maps obtained with SIRIPLAN were consistent with previous knowledge of Pantanal dynamics, but comparison with inundation extent provided by a previous satellite-based study indicates that permanently flooded areas may have been underestimated. The results obtained are promising, and further work will focus on improving vertical processes representation over floodplains and analysing model sensitivity to floodplain parameters, time step and precipitation estimates uncertainty. Copyright © 2010 John Wiley & Sons, Ltd.

KEY WORDS hydrologic modelling; hydrodynamic model; Pantanal; lateral water exchange

Received 18 March 2010; Accepted 11 October 2010

INTRODUCTION

Mathematical models have been developed and applied for simulating the hydrologic regime of rivers since the nineteenth century (Chow, 1959; Abbott, 1979; Cunge *et al*., 1981). The common approach consists of assuming that the flow is one-dimensional (1D) along the longitudinal axis of the river and employing the Saint Venant's dynamic and continuity equations for flow routing. These equations are used in their complete form (hydrodynamic model) or disregarding some terms, which give rise to the diffusive, kinematic or storage models. The choice of which model, approach and discretization to use is dependent on several factors such as the characteristics of the study area, available data sets, purposes of the study, available time, computational and human resources (Fread, 1992).

When dealing with rivers with floodplains, the two usual approaches are to consider the 1D model with extended cross sections representing both main channel and floodplain or to consider explicitly storage areas connected to the 1D model representing major water accumulation regions during floods. These methods are able to reproduce the main channel flow regime in a satisfactory way for most cases. Inundation maps may be further derived from the model results by interpolating cross sections of water levels and using a digital elevation model (DEM). However, if the study aims at representing the floodplain inundation patterns, these methods may not be suitable and a more recent approach consists of coupling a 1D model for simulating the main channel flow and a 2D model for simulating floodplain inundation (Verwey, 2001; Gillan *et al*., 2005; Hunter *et al*., 2007; Chatterjee *et al*., 2008).

Floodplain inundation plays a key role for several ecological processes and phenomena, such as ecosystem productivity, species occurrence and distribution and nutrient and sediment dynamics (Junk *et al*., 1989; Poff *et al*., 1997; Postel and Richter, 2003). Hence, being able to simulate the spatial inundation patterns through mathematical modelling provides a valuable tool to water management and prediction of climate change effects as

* Correspondence to: Adriano Rolim da Paz, Instituto de Pesquisas Hidráulicas, Universidade Federal do Rio Grande do Sul, Av. Bento Gonçalves 9500, Agronomia, CEP 91501-970, Porto Alegre-RS, Brazil. E-mail: adrianorpaz@yahoo.com.br

well the effects of human interventions such as water withdrawals, embankments, dykes and dredging projects.

In the 1D/2D coupled approach, the floodplain may be modelled by a full 2D hydrodynamic model (depth-averaged Navier–Stokes equations) or by simpler methods such as 2D diffusive and kinematic approximations. Most of the latter are regular grid models, which are commonly referred as raster-based models.

Modelling floodplain with a 2D hydrodynamic code may be infeasible due to numerical instabilities related to small water depths and the wetting and drying process as well as excessive computational costs. The use of raster-based models overcomes these difficulties and provides a way to work with a large number of floodplain grid elements. Additionally, this approach has the advantages of taking into account the spatial variability of floodplain physical characteristics (elevation and roughness) and of being easily integrated into a geographic information system (GIS). Reasonable results have been obtained by several authors with this modelling approach in terms of reproducing floodplain spatial inundation patterns (Horritt and Bates, 2001a; Bates *et al*., 2006; Wilson *et al*., 2007).

The majority of literature examples of river-floodplain modelling using the 1D/2D coupled approach encompasses relative small-scale sites (single river reaches of length less than 100 km), for which there was large amount of available data such as high-resolution DEM and inundation maps for calibrating model results (Horritt and Bates, 2001a; Bradbrook *et al*., 2004; Bates *et al*., 2006; Tayefi *et al*., 2007). The few exceptions include the study reported by Biancamaria *et al*. (2009), which modelled a single reach of 900 km length of the Ob river (Siberia), and the studies carried out by Wilson *et al*. (2007) and Trigg *et al*. (2009), which modelled a 285 km reach of the main stem of the Amazon (Solimões) river and a 107 km reach of Purus tributary. If the study site comprises an even larger and complex network of channels, junctions and floodplains (over hundreds of square kilometers), difficulties may be encountered related to data scarcity and complexity for establishing main channel and floodplain connections.

Additionally, the flood pulse may last for months long in large-scale floodplains, which considerably increase the computational cost by necessitating more model grid elements and model time steps. Moreover, for simulating these long duration floods the representation of the vertical water processes such precipitation and evapotranspiration may be required (Wilson *et al*., 2007).

In spite of the difficulties for modelling large-scale rivers and floodplains, this is the major scale of interest for assessing how climate change and variability will affect water resources. As an increase in accuracy and reliability of flow and inundation predictions is desirable for better decisions concerning land use and water management in light of climate scenarios, it motivates the development and improvement of methods for large-scale hydrologic modelling.

This paper presents a hydrologic simulation system, named SIRIPLAN, developed for large-scale river and floodplains drainage networks. This simulation system is based on coupling a 1D hydrodynamic model to a 2D raster model and considering the precipitation, evapotranspiration and infiltration processes over the floodplain. Results are presented from the application of the SIRIPLAN to the Upper Paraguay River Basin (UPRB), including the Pantanal, one of the world's largest wetlands. Results are evaluated by comparing observed and calculated hydrographs at available gauging stations and by comparing seasonal inundation areas and inundation patterns provided by previous satellite-based studies.

THE SIRIPLAN HYDROLOGIC SIMULATION SYSTEM

Overview

The SIRIPLAN hydrologic simulation system is composed by a 1D hydrodynamic model coupled to a 2D raster-based inundation model (Figure 1). The 1D model simulates the flow routing along the river drainage system, considering cross sections restricted to the main channels. The raster-based model simulates the water accumulation and the 2D propagation of inundation over the floodplains. A water exchange scheme is used to simulate the interactions between channel and floodplain. If the water level in a cross section of the main channel rises above the levee, it spills over and inundates the floodplain. Analogously, if the inundation propagation over floodplain reaches the main channel pathway, water is transferred to the channel.

Additionally, the vertical processes of precipitation, evapotranspiration and infiltration are simulated by a third module, coupled with the raster-based model. Water contributions from upstream of the modelled river drainage system are considered as boundary conditions set using

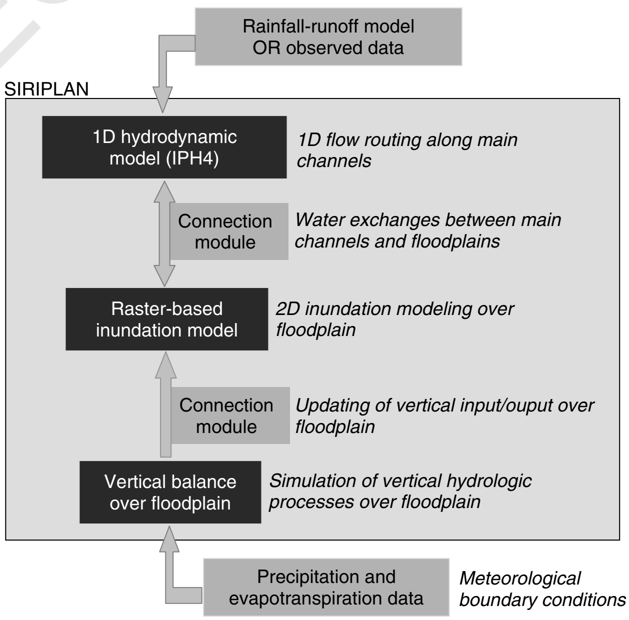

Figure 1. Conceptual overview of the SIRIPLAN hydrologic simulation system

observed discharge data or by off-line coupling of a rainfall-runoff hydrologic model.

Channel flow routing

Flow routing along main channels is simulated with the 1D hydrodynamic model called IPH4 (Tucci, 1978). This model solves the full Saint Venant equations through a finite difference method, with an implicit scheme based on a modified version of the Gauss elimination process:

$$\frac{\partial h}{\partial t} + \frac{1}{b}\frac{\partial Q}{\partial x} = q \qquad (1)$$

$$\frac{\partial Q}{\partial t} + \frac{\partial}{\partial t}\left(\frac{Q^2}{A}\right) + gA\frac{\partial h}{\partial x} + gA(S_f - S_0) = 0 \qquad (2)$$

where h is the water level, t is time, Q is the discharge, x is the longitudinal distance along the river, b and A are the cross section width and area, respectively, g is the local gravitational celerity, q is the lateral contribution to discharge per unit of distance, S_0 is the channel botton slope and S_f is the energy friction slope, which is parameterized through Manning resistance equation.

Cross-section data represented in the IPH4 model is restricted to the level which characterizes the transition between main channel and floodplain (levees). For each river reach between two cross sections, length and slope must be specified. Manning coefficients may assume distinct values for each river reach, and may also be considered variable as a function of the water level in a given cross section. The discharge exchanged between main channel and floodplains is considered as lateral contribution in the continuity equation (term q in Equation (1)).

Floodplain inundation modelling

The floodplain model is a raster-based inundation model, which was developed following the approach of the LISFLOOD-FP model (Bates and De Roo, 2000; Horritt and Bates, 2001b), but with adaptations mainly concerning the water exchange between channel and floodplain, flow among floodplain elements, water storage in soil reservoirs and water input/loss on floodplain due to vertical water balance.

Floodplain is discretized by a regular grid of interconnected elements, which may change flow with neighbouring elements and with the main channel, in the case of elements directly connected to the channel (Figure 2a). The volume variation along time in a given element of the raster model is the following:

$$\frac{\Delta V}{\Delta t_{\text{plan}}} = Q_{\text{up}} + Q_{\text{down}} + Q_{\text{left}} + Q_{\text{right}} + Q_{\text{cf}} + Q_{\text{vert}} + Q_{\text{res}} \qquad (3)$$

where ΔV is the volume variation during time interval Δt_{plan}; Q_{up}, Q_{down}, Q_{left} and Q_{right} are the discharges between the element and its up, down, left and right neighbours, respectively; Q_{cf} is the discharge between channel and floodplain element; Q_{vert} is the result of the vertical water balance and Q_{res} represents the volume of water flowing to the soil reservoir.

A numerical scheme explicit on time and progressive on space is used to solve Equation (3), considering the water level represented in the center of the element and the exchanges in its interfaces (Figure 2b). As a result, the water level in the time instant $t + \Delta t_{\text{plan}}$ in a floodplain element (i, j) is determined by:

$$^{t+\Delta t}h^{i,j} = {}^{t}h^{i,j} + \frac{({}^{t}Q_x^{i-1,j} - {}^{t}Q_x^{i,j} + {}^{t}Q_y^{i,j-1} - {}^{t}Q_y^{i,j} + {}^{t}Q_{cf}^{i,j}) \cdot \Delta t_{\text{plan}}}{\Delta x \cdot \Delta y} + {}^{t}h_{\text{vert}}^{i,j} + {}^{t}h_{\text{res}}^{i,j} \qquad (4)$$

where ${}^{t}h^{i,j}$ is the water level in time instant t, ${}^{t}Q_x^{i,j}$ is the discharge in x direction between elements i, j and $i+1$, j; ${}^{t}Q_y^{i,j}$ is the discharge in y direction between elements i, j and i, $j+1$; ${}^{t}h_{\text{vert}}^{i,j}$ is the result of the vertical water balance and ${}^{t}h_{\text{res}}^{i,j}$ is the available volume of soil reservoir, both expressed in water depth; Δx and Δy are the element dimensions in the x and y directions, respectively.

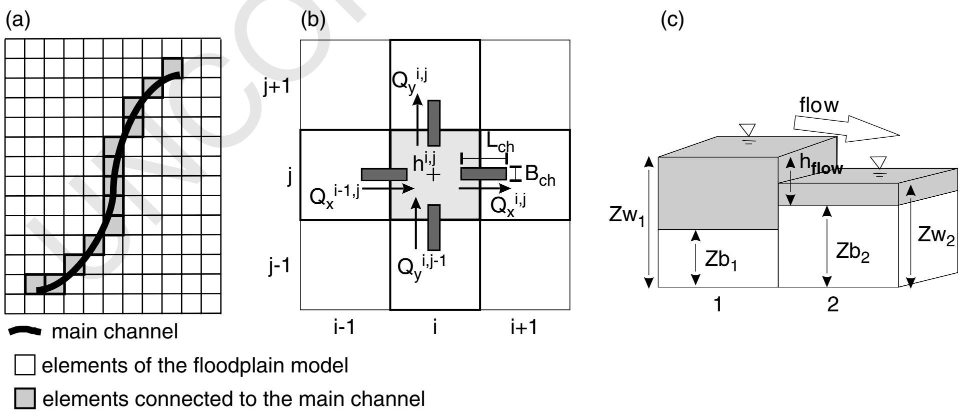

Figure 2. (a) Floodplain elements of the raster-based model; (b) numerical discretization of water level and discharges between elements of the floodplain, which are calculated through linkage channels of width B_{ch} and length L_{ch} and (c) indication of hflow between two elements (Zw and Zb refer to water level and botton elevation, respectively), where h_{flow} = Max(Zw1,Zw2)-Max(Zb1,Zb2) (adapted from Bates *et al.*, 2005)

In the soil reservoir scheme, a floodplain element is inundated, i.e. with surface water accumulation, only after the soil reservoir is full (Figure 3). The term h_{res} is given by:

$$h_{res} = h_{sub} - H_{smax} \qquad (5)$$

where h_{sub} is the current water content of the soil reservoir, which has a maximum capacity of H_{smax} (model parameter), both variables being expressed in water depth; h_{res} always assumes non-positive values, varying from $h_{res} = -H_{smax}$ when the reservoir is empty to $h_{res} = 0$ when it is full.

If the result of the water balance in a floodplain element (Equation (4)) is positive, the soil reservoir is filled and there is surface water in this element. On the contrary, a negative result means that the element was dried (in terms of surface water). The available water content in the soil reservoir is updated as follows:

$$\text{if } {}^{t+\Delta t}h^{i,j} > 0 \Rightarrow {}^{t+\Delta t}h^{i,j}_{res} = 0 \qquad (6)$$

$$\text{if } {}^{t+\Delta t}h^{i,j} < 0 \Rightarrow \left\{ \begin{array}{l} \left\{ \begin{array}{l} {}^{t+\Delta t}h^{i,j}_{res} = {}^{t+\Delta t}h^{i,j}, \text{ if } \left| {}^{t+\Delta t}h^{i,j} \right| < H_{smax} \\ {}^{t+\Delta t}h^{i,j}_{res} = -H_{smax}, \text{ if } \left| {}^{t+\Delta t}h^{i,j} \right| > H_{smax} \end{array} \right. \\ {}^{t+\Delta t}h^{i,j} = 0 \end{array} \right. \qquad (7)$$

The discharge between two neighbour floodplain elements is determined by Manning equation with a numeric and spatial discretization similar to the used by Bates and De Roo (2000). However, we consider that the flow between each two elements occurs along straight channels of width B_{ch} and length L_{ch} (Figure 2c), and thus the discharge is given by:

$${}^tQ_x^{i,j} = \pm \frac{{}^t h_{fluxo}^{5/3}}{n^{i,j}} \left(\frac{\left| {}^t h^{i,j} - {}^t h^{i+1,j} \right|}{L_{ch}} \right)^{1/2} \cdot B_{ch} \qquad (8)$$

where ${}^tQ_x^{i,j}$ is the discharge in the x direction between elements $(i,\ j)$ and $(i+1,\ j)$ in time instant t; $n^{i,j}$ is Manning roughness of the channel linking these elements and ${}^t h_{flow}$ is the water depth available to the flow between these elements; flow in y direction is determined analogously.

The water depth h_{flow} is defined as the difference between the highest water level and the highest botton elevation between the two floodplain elements (Figure 2c), following Horritt and Bates (2001a) and Bates *et al.* (2005).

When modelling large-scale floodplains, model discretization may result in elements with dimensions of hundreds or thousands of meters to reduce computational cost. If discharge along the floodplain is calculated considering the flow spilling over the whole element width, small differences in the water level may generate huge and unrealistic volumes of water exchanged between two elements, causing numerical instabilities and artificially accelerating the inundation propagation. The adoption of channels with controlled dimensions to represent the hydraulic linkage between each two floodplain elements aims at overcoming this problem. In the flow equation between elements of the floodplain, there are three parameters related to the linkage channel (Manning roughness, width and channel), which may be combined into only one, called hydraulic conductivity factor (f_{hc}) (Equation (9)). Albeit indeed inundation over large, vegetated floodplains such as Pantanal may propagate along preferential pathways, the disadvantage of the proposed approach is the increase in the number of model parameters and the difficulty to parameterize them physically. This may cause parameter equifinality, i.e. different parameter sets leading to same results (Beven and Freer, 2001). Further study may focus on evaluating model sensitivity to these parameters and the associated

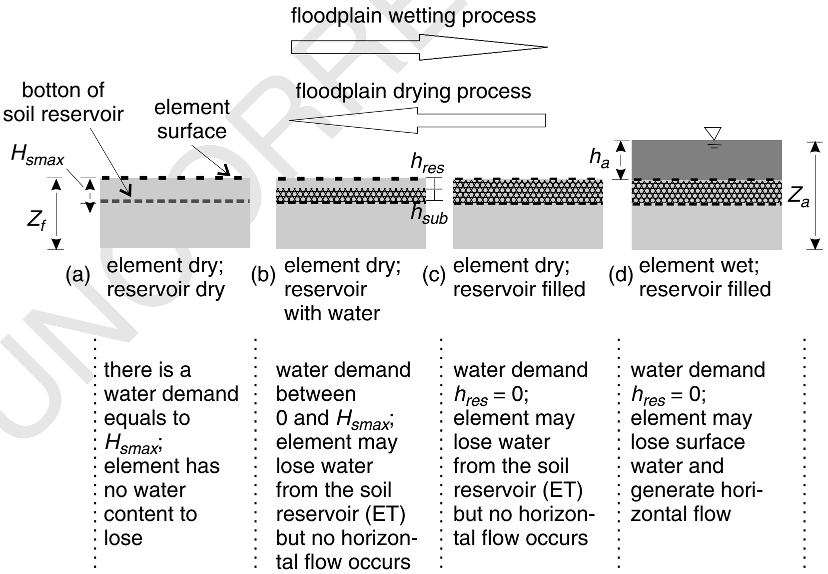

Figure 3. Wetting [(a)–(d)] and drying [(d)–(a)] processes of a floodplain element of the raster model (Z_f is floodplain elevation; Z_a is water level; h_a is surface water depth over the element; h_{sub} is water depth of soil reservoir; h_{res} is the available volume of soil reservoir, which has a maximum capacity equals to H_{smax})

uncertainties.

$$f_{\mathrm{hc}}^{i,j} = \frac{B_{\mathrm{ch}}^{i,j}}{n^{i,j}\sqrt{L_{\mathrm{ch}}^{i,j}}} \quad (9)$$

Vertical water balance on floodplain

The vertical water balance on each floodplain element is performed as a balance between precipitation and evapotranspiration. This balance is updated at a specific time step (Δt_{vert}) (Figure 4), which is commonly several times greater than time steps used in 1D and 2D models. At each Δt_{vert}, this simple water balance is calculated for a given floodplain element (i, j):

$$^{t+\Delta t}h_{\mathrm{vert}}^{i,j} = {}^{t+\Delta t}P^{i,j} - {}^{t+\Delta t}ET_{\mathrm{actual}}^{i,j} \quad (10)$$

where P is precipitation, ET_{actual} is the actual evapotranspiration and h_{vert} is the resultant of this balance, all of them expressed in terms of water depth.

If $h_{\mathrm{vert}} > 0$, it represents a source of water to the water balance of the element in the 2D model (Equation (4)), while a negative value means a sink (definite loss) of water from the modelling system. As $\Delta t_{\mathrm{vert}} >> \Delta t_{\mathrm{plan}}$, the result of the vertical balance is considered constant along the following npv number of floodplain time steps, where $\mathrm{npv} = \Delta t_{\mathrm{vert}}/\Delta t_{\mathrm{plan}}$, but after converting to corresponding units by $h_{\mathrm{vert}} = h_{\mathrm{vert}}/\mathrm{npv}$.

Actual evapotranspiration is calculated according to wet or dry condition of the floodplain element in each Δt_{vert}. If the element has surface water, actual evapotranspiration occurs at the maximum rate equal to potential evapotranspiration (Equation (11)). If the element is dry, actual evapotranspiration is less than the potential rate, being linearly proportional to water content of the soil reservoir (Equation (12)).

$$\text{if } {}^{t}h^{i,j} > 0 \Rightarrow {}^{t+\Delta t}ET_{\mathrm{actual}}^{i,j} = {}^{t+\Delta t}ET_{\mathrm{pot}}^{i,j} \quad (11)$$

$$\text{if } {}^{t}h^{i,j} = 0 \Rightarrow {}^{t+\Delta}tET_{\mathrm{actual}}^{i,j} = {}^{t+\Delta t}ET_{\mathrm{pot}}^{i,j} \cdot \left(1 - \frac{\left|{}^{t}h_{\mathrm{res}}^{i,j}\right|}{H_{\mathrm{smax}}}\right) \quad (12)$$

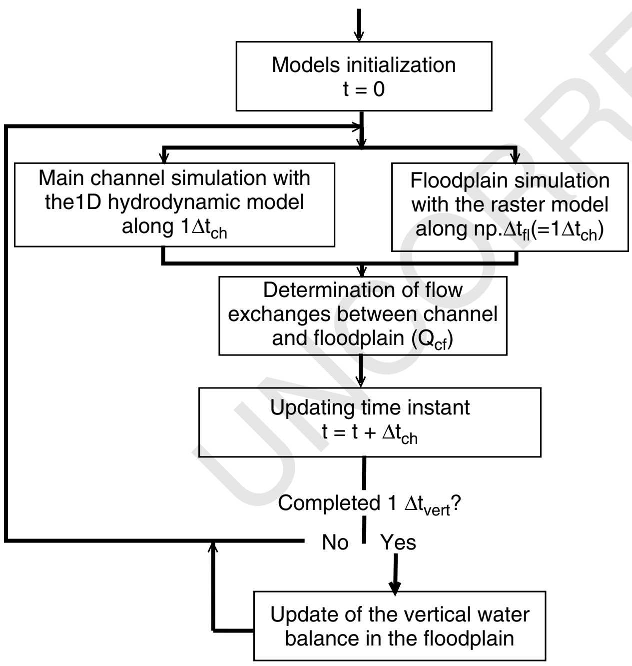

Figure 4. Scheme of coupled running of hydrodynamic and raster inundation models and vertical water balance

Channel–floodplain water exchanges

Every floodplain element located under the main channel longitudinal axis is connected with it. Water exchanges between channel and floodplain are determined as a function of the difference between water levels. For the points located between two cross sections of the main channel, the water level is calculated by a linear approximation.

Occurrence of flow between channel and floodplain in a given location is triggered by the condition of water level in floodplain and/or main channel higher than the spill elevation (Z_{spill}). This elevation is the maximum value between channel levee height and floodplain bottom elevation.

When the water level in the main channel or in the floodplain reaches Z_{spill}, there is hydraulic connection and flow occurs. This flow is calculated using simple or flooded weir-type equations. Analogously to the discharge between floodplain elements, if the weir width is considered equal to the element width, unrealistic exaggerated flow may be calculated for small water depths over the weir in case of elements with large dimensions. Therefore, the weir width is considered a model parameter, usually taken in the range 10–100 m, which may be regarded as the typical width values over which occurs lateral flows in large natural rivers. As previously stated regarding parameters related to channels linking floodplain elements, considering the weir width as a model parameter may lead to equifinality and increase the uncertainties. Further study will evaluate this issue, investigating model sensitivity to each parameter.

A decoupled 1D/2D time-step approach is considered (Trigg *et al.*, 2009), in which different time steps are set to the 1D and 2D models. The 1D time step (Δt_{chan}) is usually several times greater than the 2D time step (Δt_{plan}), as the 1D model uses an implicit numeric scheme while the 2D model is explicitly solved. Thus, the 1D model is run by $1\Delta t_{\mathrm{chan}}$ and then the 2D model is run by np times Δt_{plan}, where $\mathrm{np} = \Delta t_{\mathrm{chan}}/\Delta t_{\mathrm{plan}}$. After a time interval of Δt_{chan}, the water exchanges (Q_{cf}) between channel (1D model) and floodplain (2D model) are calculated. For the channel, Q_{cf} is converted into lateral contribution to discharge per unit of distance for calculation of the continuity equation (Equation (1)) at the next Δt_{chan}. For the floodplain, Q_{cf} is directly used into the water level updating equation (Equation (4)) throughout a time interval of Δt_{chan}, i.e. for the next np Δt_{plan}.

Code and parallelization

The SIRIPLAN hydrologic simulation system was developed using FORTRAN 90 programming language and OpenMP (Open specifications for Multi-Processing) Application Programming Interface (API). The OpenMP represents a collection of directives, library routines and environment variables that enables programs to run in parallel on shared memory processors (Hermanns, 2002; Chapman *et al*., 2008). The main advantages of this approach relative to other parallel techniques are the ease of implementation and requirements of minimal modification to the code. Recently, Neal *et al*. (2009) implemented a parallel version of the LISFLOOD-FP model using OpenMP, achieving parallel efficiencies of up to 0·75 on four and eight processor cores.

Two loops of the raster inundation model were parallelized through OpenMP: the calculation of discharge between floodplain elements and the calculation of water depth in each element (general water balance). The 1D hydrodynamic model has an implicit numerical scheme, and tests for parallelizing its code with OpenMP has proven not to be advantageous in terms of run-time reduction (Paiva, 2009).

INPUT DATA REQUIREMENTS AND PREPARATION

Main channel data

For the hydraulic modelling of channel flow, data requirements includes channel vector lines, length and slope, cross section profiles and boundary conditions. Among these data, the profiles are the most difficult to obtain. To overcome this issue, a simple linear scheme is adopted for cross-section profiles interpolation when necessary. Given an upstream and a downstream section with available profiles, for each intermediate cross section to be created, the horizontal and vertical location of its *i*th point is determined through linear interpolation of the *i*th upstream and downstream points.

Main channel georeferenced vector lines may be obtained from available maps or by digitizing satellite images, while length and slope of main channels are derived from cross-section data and channel vector lines, taking into account a floodplain DEM as auxiliary data.

Floodplain data

The raster-based model requires a floodplain mask and a DEM to represent floodplain topography. The mask defines the modelled domain, which is established based on the main channel network, floodplain topography and contributing drainage areas of the boundary conditions of the channels. As a no flow boundary condition is imposed to the floodplain in the raster model, the floodplain mask must comprise the full extent of the inundation area. Areas which certainly are not flooded and which do not significantly contribute to flooding may be excluded from floodplain domain to reduce computational cost.

Additionally, precipitation and potential evapotranspiration data are required for the vertical water balance on floodplain. Point specific data such as rainfall gauging station observations or data provided by other sources such as precipitation estimates from atmospheric models are interpolated to the raster model grid using the inverse distance square method. This procedure is carried out before simulation to reduce model run time. These data are required with a discretization on time equal to Δt_{vert}. Alternatively, seasonal monthly estimates of potential evapotranspiration may be used if more detailed data are not available.

Channel–floodplain connection

The largest effort on input data preparation involves establishing the topological connections between channel and floodplain discretization elements. This is not a trivial task when dealing with several tributaries, junctions and hundreds of cross sections, and where the large dimensions of the floodplain elements contrast with relative small channel meanders.

The main channel drainage network must be represented in terms of raster model grid elements, identifying which floodplain elements are connected to each channel reach, and which cross section or intermediate point of the reach is connected to each element. A four-step procedure was developed to accomplish this task.

The first step is the conversion of vector channel network to raster format with spatial resolution and extent equal to the floodplain discretization (Figure 5a). The resulting image is composed by pixels representing or not the channel network (Figure 5b).

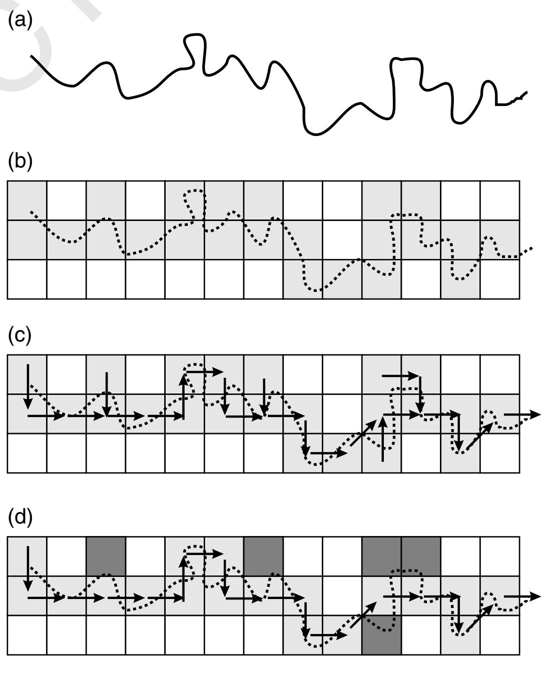

Figure 5. (a) Main channel vector drainage (VD); (b) VD converted to raster (grey pixels); (c) flow directions and (d) raster drainage with a unique pixel-to-pixel flow path (dark pixels were excluded from the original raster drainage)

Derivation of flow directions is the second step (Figure 5c). Considering the set of non-zero pixels as a mask, the direction water flows out of each pixel is determined based on floodplain DEM, through the well-known D8 (deterministic eight-neighbour) algorithm (Mark, 1984; Burrough and McDonnel, 1998; Jenson and Domingue, 1988). This algorithm approximates the local flow direction by the direction of the steepest downhill slope within a 3 × 3 window of pixels over a raster DEM. As this algorithm has a tendency of generating parallel drainage paths on flat areas, a stochastic factor as proposed by Fairfield and Leymarie (1991) was introduced to lessen this problem.

Thirdly, starting from the most upstream pixel of each channel reach, trace the downstream path following flow directions and mark every pixel reached. These marked pixels form the main channel network representation in terms of a unique pixel-to-pixel flow path. Pixels non-marked are eliminated from the raster representation of main channels (Figure 5d).

Every floodplain element corresponding to the raster pixel-to-pixel channel network is connected with main channel, while none of the other elements are connected. The fourth step is the identification of to which cross section each element is associated.

The cross sections with available profile and geographic coordinate data are associated to the pixel corresponding to these coordinates. For the interpolated cross sections, albeit their longitudinal position along the main channels is known, a rescaling procedure is performed before locating them, due to the tendency of underestimating distances on a coarse-resolution raster representation of meandering channel networks (Fekete *et al*., 2001; Paz *et al*., 2008).

The distances along the raster channel representation are measured between each of the cross sections already located. The flow path is followed pixel by pixel, summing a distance equal to pixel side for an orthogonal step and equal to 1·414 times pixel side for a diagonal step. For each reach defined by two of these cross sections, the ratio between the distances measured on the raster and on the vector drainages is calculated. This ratio is applied to convert the longitudinal position along the main channel of the interpolated cross sections into distances along the raster channel representation, defining the location of these sections.

EXAMPLE OF APPLICATION: UPRB

Site description and simulation period

The study site comprises the Pantanal area of the UPRB that has an estimated drainage area of 600 000 km^2, extending over three South American countries (Figure 6): Brazil, Paraguay and Bolivia. The UPRB is part of the La Plata basin and has three distinct regions: Planalto (260 000 km^2), Pantanal (140 000 km^2) and Chaco (200 000 km^2). The Planalto region encompasses the uplands of the basin mainly in the North and East portions. Located in the West part of the UPRB, the Chaco is a region characterized by low annual rainfall and an endorheic and undefined drainage system.

The Pantanal region is located in the central portion of the UPRB and presents very low and flat relief, with a complex drainage system. Rivers seasonally inundate the floodplains and flood waters create an intricate drainage system, including vast lakes, divergent and endorheic drainage networks. Annual rainfall is less than the potential evaporation and drainage is very slow because of shallow gradients (Bordas, 1996; Tucci *et al*., 1999).

The Pantanal region was modelled with the SIRIPLAN hydrologic simulation system, considering the contribution of the Planalto area as boundary condition, as floodplain inundation is negligible in this part of the basin. The Chaco region was not modelled due to data scarcity and because its contribution to Paraguay River is considered insignificant (Tucci *et al*., 2005). A period of 11 years and 4 months from 1 September 1995 to 31 December 2006 was selected for simulation, as this is a more recent period with reliable available data (•Table I).

The Pantanal is considered one of the largest wetlands of the world, with extraordinary biodiversity (Harris *et al*., 2005) and of great global ecologic value (Pott and Pott, 2004; Junk *et al*., 2006). Modelling its hydrologic regime and floodplain dynamics is imperative for understanding, predicting and mitigating possible effects of anthropogenic activities that currently threaten its integrity, such as dam building, agriculture and cattle raising (Tucci and Clarke, 1998; Hamilton, 1999; Hamilton *et al*., 2002; Da Silva and Girard, 2004; Junk and Cunha, 2005).

1D hydrodynamic model application

The river drainage system modelled with the 1D hydrodynamic model covers 3965 km of river channels: 1250 km of the Paraguay River and 2715 km of its main tributaries. The flow path of each channel was obtained by manually digitizing Landsat7 ETM+ satellite images.

For the Paraguay River, a total of 288 detailed cross-section profiles was available, with distances between consecutive profiles varying from 0·5 to 10 km. On the contrary, only 19 profiles were available for all the tributaries together and a linear interpolation procedure was performed to generate profiles at about 5 km intervals. Further information concerning river morphology and slopes available in former studies (DNOS, 1974; Brasil, 1997; Tucci *et al*., 2005) as well as elevation values extracted from SRTM-90m DEM were used as auxiliary data for the vertical positioning of cross sections. Detailed description of data preparation for cross sections is presented in Paz *et al*. (2010).

Streamflow gauging stations with available observed discharge time series were defined as the upstream boundary conditions of the 1D hydrodynamic model. Missing data were replaced by values calculated with the distributed hydrologic model MGB-IPH (Collischonn *et al*., 2007). This model was previously applied and

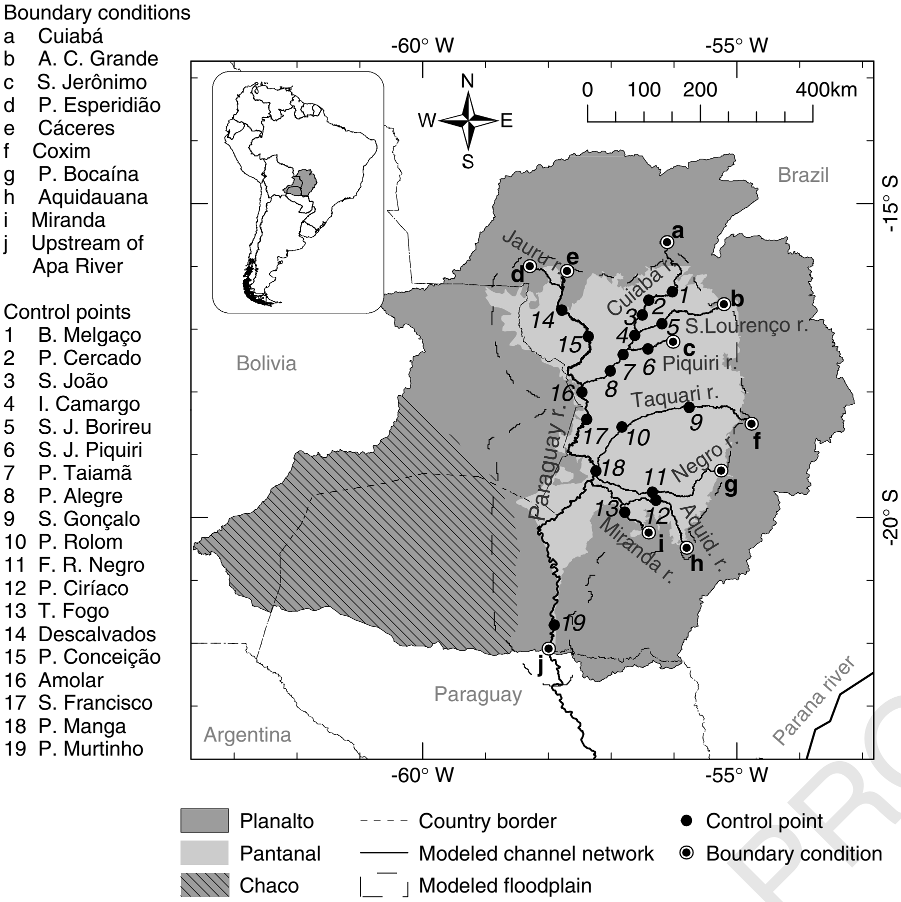

Figure 6. Location of Upper Paraguay River Basin and indication of modelled channel network and floodplain, and of streamflow gauging stations used as control points or boundary conditions

Table I. List of boundary conditions with drainage area and observed daily discharge data availability during the simulation period (1 September 1995–31 December 2006)

Streamflow gauging station defining the boundary condition (reference to Figure 6)		River	Drainage area (km^2)	Observed discharge data availability (% of simulation period)[a]
a	Cuiabá	Cuiabá	24 668	100
b	A. C. Grande	S. Lourenço	23 327	94
c	S. Jerô nimo	Piquiri	9215	99·7
d	P. Espiridião	Jauru	6221	96·5
e	Cáceres	Paraguay	32 574	96·4
f	Coxim	Taquari	28 688	99·5
g	P. Bocaína	Negro	2807	0
h	Aquidauana	Aquidauana	15 350	97·1
i	Miranda	Miranda	15 502	99·7
j	• Upstream of Apa River[b]	Paraguay	594 092	[b]

AQ1

[a] Data available from the Brazilian Water Agency (ANA).
[b] Downstream boundary condition defined by the Paraguay River section upstream of the affluence of Apa river, considering the energy slope parallel to average bed slope.

adjusted for all the sub-basins of the Planalto region of the UPRB in the study reported by Tucci *et al*. (2005). A very reasonable fit of the MGB-IPH model was achieved by these authors, with Nash–Suttcliffe (NS) coefficients ranging from 0·56 to 0·88.

The Paraguay River section upstream of the affluence of Apa River, about 60 km downstream from Porto Murtinho, was taken as the downstream boundary condition of the modelled network, considering the energy slope parallel to average bed slope. The time step of channel flow modelling (Δt_{chan}) was adopted as 1 h, and the initial conditions were determined considering steady backwater flow approximation.

2D raster-based model application

The floodplain modelled area was defined according to earlier studies that delimited the Pantanal and the SRTM-90m DEM, but also taking into account that a no flow boundary condition is imposed to the raster model. For this reason, the modelled area was traced overestimating the area subject to inundation, which is roughly about 140 000 km^2. The raster model domain comprises 219 514 km^2 (Figure 6), discretized into 46 741 elements on a 0·02° × 0·02° grid. In planar units, each element is approximately 2 km wide, with surface area ranging from 4·58 to 4·78 km^2 depending on its latitude.

Floodplain topography was represented by the SRTM-90m DEM resampled to the raster-based model discretization, using the nearest neighbour interpolation method. Following the data preparation procedures, a total of 1081 floodplain elements were identified as directly connected to the main channels.

The inundation model was run with a 120-s time step, which was selected after testing different values and verifying that this value avoided numerical instabilities. A 1-day time step was selected for the vertical water balance, due to precipitation and potential evapotranspiration data availability on a daily basis and also because this is adequate to represent the modelled processes in this study area. Observed precipitation data available from 105 rainfall gauging stations were interpolated to the 0·02° grid resolution of the floodplain model using the inverse distance squared method. Although this rain gauge network is sparse, for instance it is sufficient to provide precipitation estimates for testing the proposed model. Future work will try to investigate model sensitivity to precipitation estimates and also the combination of pluviometer measures with satellite-based estimates, such as those generated by the Tropical Rainfall Measuring Mission (TRMM; Kummerow *et al*., 2000).

The estimates of potential evapotranspiration produced by the MGB-IPH distributed hydrological model applied to the entire UPRB in a earlier study (Tucci *et al*., 2005) were used as input data. The MGB-IPH model calculates potential evapotranspiration through Penman–Monteith method as presented by Shuttleworth (1993) and following the approach proposed by Wigmosta *et al*. (1994). Distinct combinations of land cover and soil type are represented inside each model cell through patches with specific parameter values. This model was applied to the UPRB considering a 0·1° × 0·1° regular grid and a 1-day time step. The simulation period was from 1968 to 2006, and the estimates of potential evapotranspiration used as input data for the floodplain model correspond to the patch representing surface water, which were interpolated to the 0·02° floodplain model grid using the inverse distance squared method.

Calibration procedure and model skill assessment

To evaluate the performance of the 1D hydrodynamic model, 15 streamflow gauging stations with available data were used as control points for comparing calculated and observed discharges along the main channel network (Figure 6). Floodplain inundation dynamics simulated by the raster model was compared with estimates of total inundated area provided by Hamilton *et al*. (1996) and with estimates of inundation extent produced by Padovani (2007).

Hamilton *et al*. (1996) estimated the total of flooded areas of Pantanal in the period 1979–1987 through analysis of data obtained by the scanning multichannel microwave radiometer (SMMR) sensor of the Nimbus-7 satellite. Despite the related uncertainties mostly due to coarse resolution of satellite images (27 km), vegetation cover heterogeneity, and of being relative to a time period distinct from the one simulated in this article, the study of Hamilton *et al*. (1996) presented to date the most complete time series of seasonal floods in the Pantanal.

Padovani (2007) classified images of the sensor wide-field imager (WFI) on board of the CBERS-2 satellite (China–Brazil Earth Resources Satellite) to distinguish between flooded and non-flooded areas of Pantanal for the dates 6 October 2004 (dry period) and 13 February 2005 (wet period). These images have a spatial resolution of 260 m and, as the WFI has a ground swath of 890 km, a unique scene covering the entire area of interest for each date was used (path 165, row 116). These images were classified by an unsupervised method, the Iterative Self-Ordering Data Analysis (ISODATA) algorithm, as implemented in the ERDAS Imagine 8·5 software. The resulting classes were grouped into flooded or non-flooded areas, taking the RGB color composite of Landsat 7 ETM+ images for the year 2000 and digital aerial photographs of the region as ancillary data. Undoubtedly these estimates have uncertainties, mostly associated to inundated areas covered by vegetation and areas with wet saturated soil, which may lead to under- and overestimation of flooded extent, respectively. However, this is the only readily available inundation extent mapping of the entire Pantanal area for comparison with our results.

A simplified approach was adopted for adjusting model parameters, as the calibration process of coupled 1D/2D models is not straightforward. For instance, some studies indicate that it is not possible to find a unique set of parameters of the raster model that provide acceptable adjustments for both channel flow and floodplain inundated area (Horritt and Bates, 2001b). •Another question concerns whether using constant or spatially varying parameters on 2D floodplain models (Werner *et al*., 2005; Hunter *et al*., 2007). Albeit several efforts have been conducted to estimate friction parameters based on remote sensing data (Bates *et al*., 2004), in the case of simplified models, such as the proposed in this article, the parameters are related to aggregated hydraulic process descriptions (Hunter *et al*., 2007), weakening the relation of them with floodplain physical characteristics. In light of this discussion and due to the large extent of the study case and scarce available data sets, in this study the calibration process focused primarily on reproducing main channel flow, but also trying to reproduce general aspects of floodplain dynamics. Further study may focus particularly on adjusting model parameters for reproducing inundation patterns.

AQ3

Initially, a constant Manning coefficient was adopted for all main channel reaches in the 1D hydrodynamic model, and several runs of the hydrologic simulation system were performed with varying floodplain model parameter values. The Manning channel roughness was selected as 0·035 following a recommendation for large natural rivers (Chow, 1959, 1964). The parameters $f_{\rm hc}$ and $H_{\rm smax}$ were varied in each simulation run, but assuming constant values along the floodplain.

This rough sensitivity analysis of floodplain parameters lead to the selection of the values $f_{\rm hc} = 50$ and $H_{\rm smax} = 1{\cdot}0$ m, based on channel hydrograph comparisons and the modelled general inundation patterns, both in terms of total inundated area and inundation extent. Adopting these values for the floodplain parameters, a new set of simulation runs was carried out for adjusting main channel roughness. This was done in a trial and error process, by manually varying the Manning coefficient values and comparing calculated and recorded hydrographs through visual inspection and using as statistical measures the NS model efficiency coefficient (NS), the NS coefficient for logarithms of discharge values (NSlog), the relative streamflow volume error (ΔV) and the root mean square error (RMSE). The calibration procedure was realized first for the tributaries and then for the Paraguay River, from upstream to downstream along each river.

Finally, assessment of floodplain inundation dynamics, through comparison with results of Hamilton *et al.* (1996) and Padovani (2007), was carried out considering the simulation run using the adjusted main channel Manning coefficients and the selected values for floodplain parameters. It is worth noting that those authors considered distinct delimitations for defining the Pantanal area in their studies, albeit in general these delimitations are very similar between them. The Pantanal's area following the outline of Hamilton *et al.* (1996) is about 138 139 km^2, while the one used in the study of Padovani (2007) has 138 437 km^2. The major difference between them regards to the west portion, where the delimitation used by Padovani (2007) follows the Brazilian country border, as this sketch defines the Pantanal region officially adopted by Brazilian Government.

Simulated total inundated area was converted into average seasonal values for comparison with the results of Hamilton *et al.* (1996), considering the Pantanal delimitation adopted by those authors and adopting the depth threshold of 2 cm to distinguish between dry and inundated condition of each element of the raster-based model.

The comparison between simulated and Padovani's estimates of inundation extent was carried out through a pixel-to-pixel basis, and considering the Pantanal delimitation used by that author. We aggregated the 260 m inundation maps of Padovani (2007) to the spatial resolution of the raster-based model (2 km). Each pixel of the Pantanal area was compared whether wet or dry on both simulated and estimated inundation maps. A 2 × 2 contingency table was built as shown in Figure 7, where 'a'

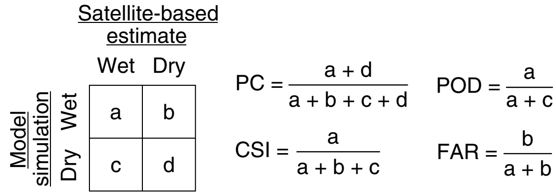

Figure 7. Contingency table (2 × 2) for comparison between inundation maps resultant from satellite-based estimates and floodplain model simulation, where 'a' and 'b' are the number of pixels which were wet on both maps, 'c' is the number of pixels which were wet on estimated map but dry on simulated map and 'd' is the number of pixels which were dry on estimated map but wet on simulated map; and four derived skill scores: proportion correct (PC, critical success index (CSI, probability of detection (POD and false alarm ratio (FAR)

and 'd' correspond to the number of wet and dry pixels, respectively, simultaneously on both simulated and estimated maps. The number of pixels which were estimated as wet but simulated as dry are summed in 'c', while 'd' is the number of pixels that were wrongly simulated as wet (they were estimated as dry). Four skill scores were then derived: proportion correct (PC), critical success index (CSI), probability of detection (POD) and false alarm ratio (FAR) (Figure 7). Each of these measures of fit suggests distinct analysis of the results (Wilks, 2006).

The index PC is simply the fraction of the total amount of pixels in agreement between model simulation and Padovani's estimate, indistinctly whether wet or dry. It ranges from 0 (no agreement) to 1 (perfect agreement), and means the area correctly predicted by the model. For instance, the PC was used as a measure of fit of inundation models by Bates and De Roo (2000) and Pearson *et al.* (2001).

The CSI is similar to PC, but accounting for only the agreement of wet pixels and disregarding the correct simulation of dry pixels, under the assumption that it is relatively easier to correctly predict non-flooded areas. The CSI may also be interpreted as the ratio between the intersection of simulated and estimated flooded areas and the combination of them. It ranges from 0, when no overlap occurs between flooded areas of simulated and estimated inundation maps, to 1, when there is exactly a coincidence. This is by far the most widely used measure of fit for evaluating simulated inundation extent against estimates from others sources (Bates and De Roo, 2000; Horritt and Bates, 2001a; Bates *et al.*, 2005; Tayefi *et al.*, 2007; Wilson *et al.*, 2007).

The POD skill score, also known as hit rate, means the fraction of the pixels estimated as wet which were correctly simulated as so, ranging from 0 to 1 (the higher the value the better the performance). The FAR means the fraction of the pixels estimated as dry which were wrongly simulated as wet, also ranging from 0 to 1, but the smaller the value the better the performance. These indices are mostly used for comparing spatial fields of precipitation and other meteorological variables (Wilks, 2006), but also provide interesting analysis for floodplain inundation assessment.

RESULTS AND DISCUSSION

Computation time and performance

To evaluate the gain of introducing the parallelization scheme via OpenMP for part of the floodplain model, the SIRIPLAN was run for the UPRB in a sequential mode and further considering two and four processor cores in the parallelization. The three runs were performed in a quad core Intel processor 3 GHz with 4 GB RAM.

The computation time required in each run is shown in Table II. When running sequentially, the run time was greater than 4 h. This run time was reduced by 45% when adopting a two cores parallelization and by 67% when parallelizing with four cores. Parallel speedup (run time of parallel execution divided by run time of sequential execution) equal to 1·82 and 3·07 was obtained for two and four cores parallelization, respectively. In terms of parallel efficiency (speedup divided by the number of processor cores), running in parallel with two and four cores resulted in values of 0·91 and 0·77, respectively.

The values of parallel speedup and efficiency obtained with SIRIPLAN in this study were similar to the best results presented by Neal *et al*. (2009), who ran the LISFLOOD-FP model applied to several different study cases considering the OpenMP parallelization technique.

Flow regime along main channels

A very reasonable model fit was obtained in terms of reproducing main channel flow along the Paraguay River and its tributaries, as indicated by the performance measures comparing observed and calculated hydrographs shown in Table III, relative to the period from 1 December 1997 to 31 December 2006 (the antecedent period was disregarded due to initial conditions influence).

For the gauging stations located at the tributaries, the adjusted Manning coefficients ranged from 0·02 to 0·055, and were obtained NS and NSlog coefficients ranging from 0·75 to 0·94 and from 0·80 to 0·97, respectively. The volume error for these stations was less than 10% in absolute value, except for the Ilha Camargo station ($\Delta V = -13{\cdot}5\%$), while the RMSE ranged from less than 20 m^3/s at P. Ciríaco (Aquidauana River) to near 100 m^3/s at P. Taiamã (Cuiabá River).

The model was capable to reproduce the general shape of observed hydrographs at the tributaries, as illustrated by visually comparing observed and calculated hydrographs at P. Cercado, P. Taiamã and P. Ciríaco gauging stations (Figure 8a–c, respectively). For instance, these three cases exemplify the complexity of flow regime of rivers flowing along Pantanal. There is a small overestimation trend on calculated seasonal peak flows at P. Cercado station, of about 10% for the wettest years, while at P. Taiamã and P. Ciríaco there is an underestimation trend of up to 15% and 5% on calculated seasonal peak flows, respectively. For these three gauging stations, there are insignificant differences between observed and calculated recession flows.

Table II. Run time and performance of the SIRIPLAN hydrologic system applied to the Upper Paraguay River Basin

Run type	Run time	Performance relative to single core		
		Run-time reduction	Speedup	Efficiency
Sequentially	4 h 23 min 47 s	—	—	—
Parallel two cores	2 h 25 min 10 s	45%	1·82	0·91
Parallel four cores	1 h 26 min 25 s	67%	3·07	0·77

Table III. Performance measures of SIRIPLAN hydrologic system in simulating main channel flow along Paraguay River and its tributaries

Reference to Figure 6	Station names	River	Drainage area (km^2)	Statistics[a]			
				RMSE (m^3/s)	NS	NSlog	ΔV (%)
1	B. Melgaço	Cuiabá	27 050	70·2	0·94	0·97	−5·8
2	P. Cercado	Cuiabá	38 720	46·1	0·91	0·92	−4·6
3	S. João	Cuiabá	39 908	50·2	0·82	0·84	−8·8
4	I. Camargo	Cuiabá	40 426	85·3	0·78	0·80	−13·5
5	S. J. Borireu	S. Lourenço	24 989	26·6	0·92	0·94	4·9
6	S. J. Piquiri	Piquiri	28 871	89·2	0·75	0·82	8·9
7	P. Taiamã	Cuiabá	96 492	98·5	0·90	0·92	−2·1
8	P. Alegre	Cuiabá	104 408	79·8	0·82	0·85	8·3
9	P. Ciríaco	Aquidauana	19 204	18·0	0·76	0·83	−3·5
10	Descalvados	Paraguay	48 360	79·3	0·91	0·92	−5·0
11	P. Conceição	Paraguay	65 221	80·1	0·63	0·62	7·6
12	Amolar	Paraguay	246 720	180·7	0·67	0·72	6·3
13	P. S. Francisco	Paraguay	251 311	258·7	0·70	0·73	−2·0
14	P. Manga	Paraguay	331 114	191·3	0·82	0·76	2·5
15	P. Murtinho	Paraguay	581 667	343·5	0·61	0·65	−6·1

[a] To exclude the effect of initial conditions, statistics were calculated for the period from 1 December 1997 to 31 December 2006.

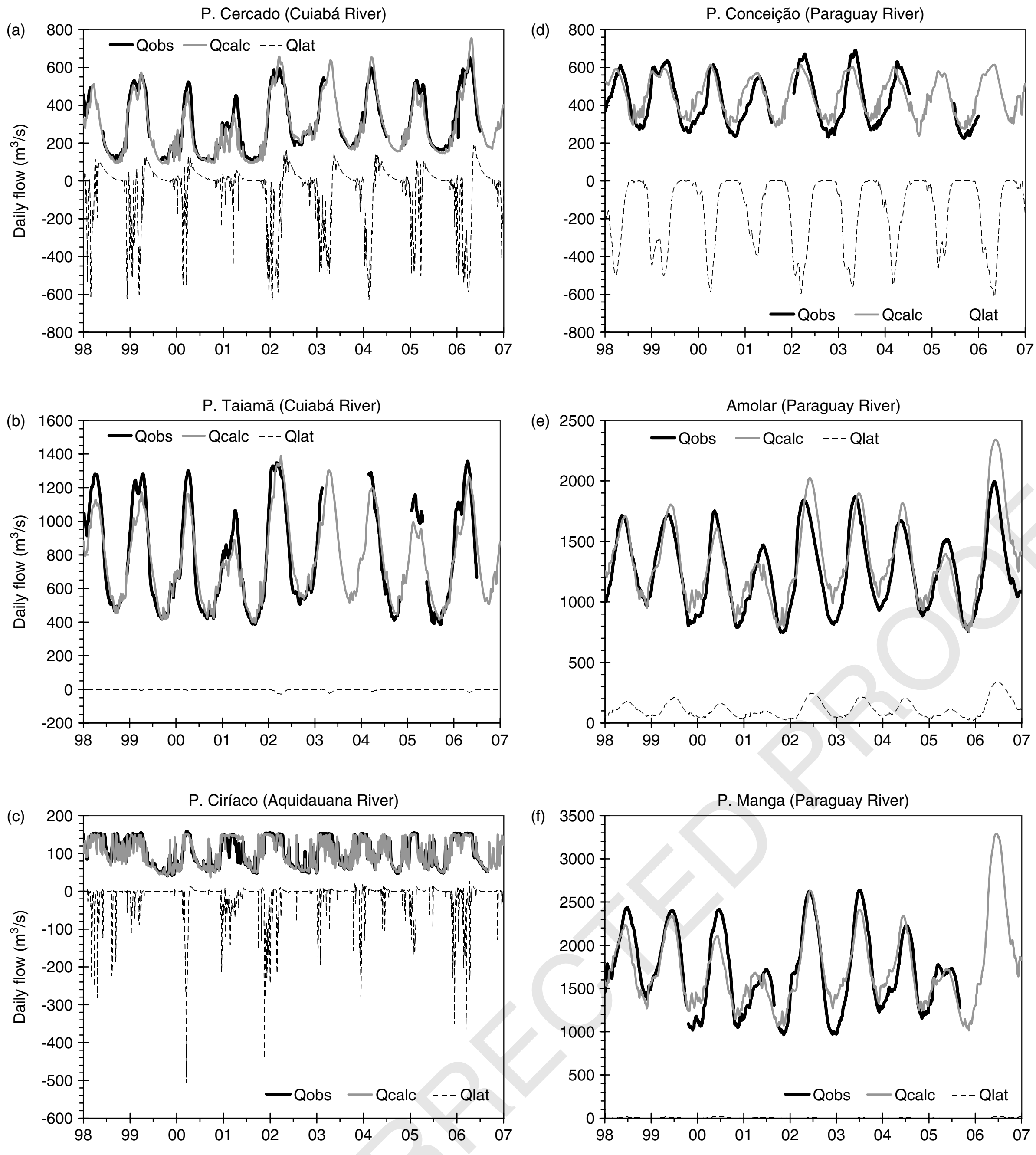

Figure 8. Comparison of calculated (Qcalc) and observed (Qobs) hydrographs at three gauging stations located at tributaries and three stations of Paraguay river; Qlat is the lateral flow exchanged between main channel and floodplain along the following river reaches: (a) from B. Melgaço to P. Cercado; (b) from the confluence of Piquiri and Cuiabá Rivers to P. Taiamã; (c) from Aquidauana to P. Ciríaco; (d) from Descalvados to P. Conceição; (e) from the confluence of Cuiabá and Paraguay Rivers to Amolar and (f) from P. S. Francisco to P. Manga; Qlat <0 means flow from main channel to floodplain and Qlat >0 means flow in the opposite direction

In the graphs of Figure 8, Qlat means the calculated lateral flow exchanged between main channel and floodplain along the upstream river reach specified on the caption of the figure for each case, being negative if flowing from the channel to floodplain and positive if flowing in the opposite direction. Along the 107 km reach of Cuiabá River upstream of P. Cercado, was simulated a huge loss of water from channel to floodplain during rising limb of flood hydrograph, with Qlat achieving up to -600 m^3/s (around 8% greater than flood peak along main channel), and a gain of water after flood peak flow of up to 180 m^3/s. Meanwhile, no water exchanges between channel and floodplain were simulated for the river reach upstream of P. Taiamã station.

At P. Ciríaco station, located on the Aquidauana River 230 km downstream from Aquidauana station (boundary condition), the observed hydrograph presents a marked maximum value of 150 m^3/s. At Aquidauana station, observed peak flow reaches up to 700 m^3/s. This enormous reduction of channel flow in this river reach was well represented by the model, which simulated lateral exchanges of water from channel to floodplain of

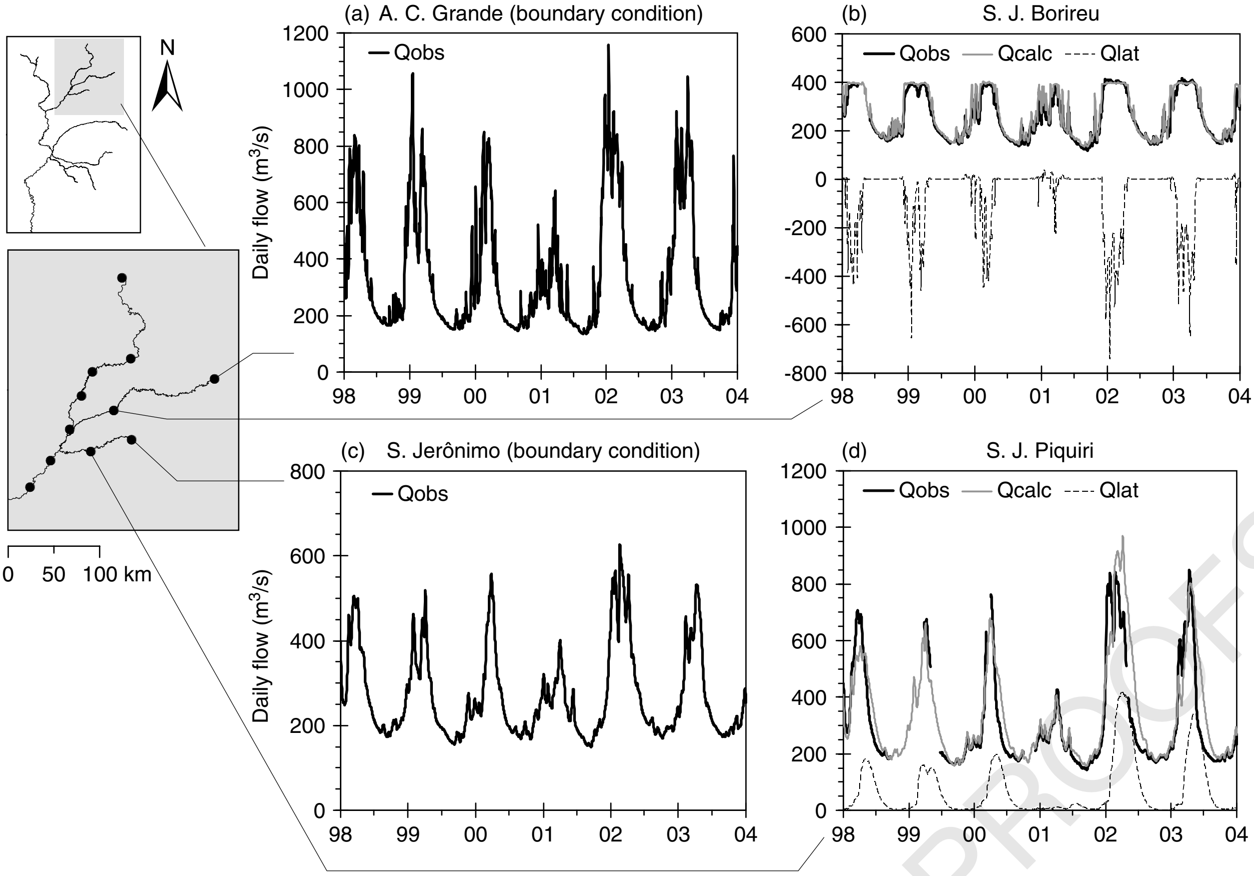

Figure 9. (a) and (c) Observed hydrographs at the boundary conditions of S. Lourenço (A. C. Grande station) and Piquiri (S. Jerônimo) rivers and (b) and (d) comparison between calculated (Qcalc) and observed (Qobs) hydrographs at their downstream gauging stations, also showing lateral flow exchanged between main channel and floodplain along each river reach between the boundary condition and the downstream station

up to 500 m^3/s during flood peaks. The maximum lateral discharge simulated corresponds to 3·3 times peak flow along main channel at P. Ciríaco. During the dry period, no water drainage from the floodplain was simulated and the observed recession flow at this station was also well reproduced.

As at P. Ciríaco, a marked maximum flow (of about 400 m^3/s) on observed hydrograph is also seen at S. J. Borireu station, located on the S. Lourenço River, which was well reproduced by the model (difference less than 5%) (Figure 9a and b). Along the 250 km long reach between this station and the upstream boundary condition (A. C. Grande station), the model simulated lateral flows of up to 750 m^3/s from main channel to floodplain.

In the reach of the Piquiri River upstream of S. J. Piquiri station (80 km downstream from S. Jerônimo, taken as boundary condition), the exchanges of water between floodplain and main channel was simulated as occurring in the opposite direction of that reported to the S. Lourenço River (Figure 9c and d). A gain of water from the floodplains to the main channel was simulated in this reach of Piquiri River, totalling up to 400 m^3/s during the floods. This gain of water represents almost 50% of the water flowing along the main channel at S. J. Piquiri station. In fact, while at S. Jerônimo observed peak flow ranges between 400 and 700 m^3/s, at S. J. Piquiri this range is between 400 and 1100 m^3/s. The increase in observed peak flow from upstream to downstream is due to lateral floodplain contribution, which the model was capable to simulate. The estimated hydrograph of this lateral gain of water to main channel presents a small time delay relative to channel flood peak. During dry periods, this hydrograph reached null values, which allowed recession flow at S. J. Piquiri to be quite well reproduced. Most interestingly is that the major part of the contribution of floodplain to main channel of Piquiri River at this location during floods was resultant from the volume of water lost by the main channel of the S. Lourenço River, 35 km to North, which flowed along floodplains.

Owing to large drainage areas and complexity of processes involved, including contributions of tributaries that may occur both through main channel and floodplain flows, reproduction of flow regimes along the Paraguay River is even more difficult than along its tributaries. However, the model was able to reproduce the seasonal flow regime along the Paraguay River, as illustrated by the performance measures comparing observed and calculated flows at six gauging stations (Table III). The NS and NSlog coefficients ranged from 0·61 to 0·91 and from 0·62 to 0·92, respectively. RMSE were obtained between 80 and 343 m^3/s, which seem to be large errors in absolute terms, but correspond roughly to less than 13% of average peak flow in each station: 7%

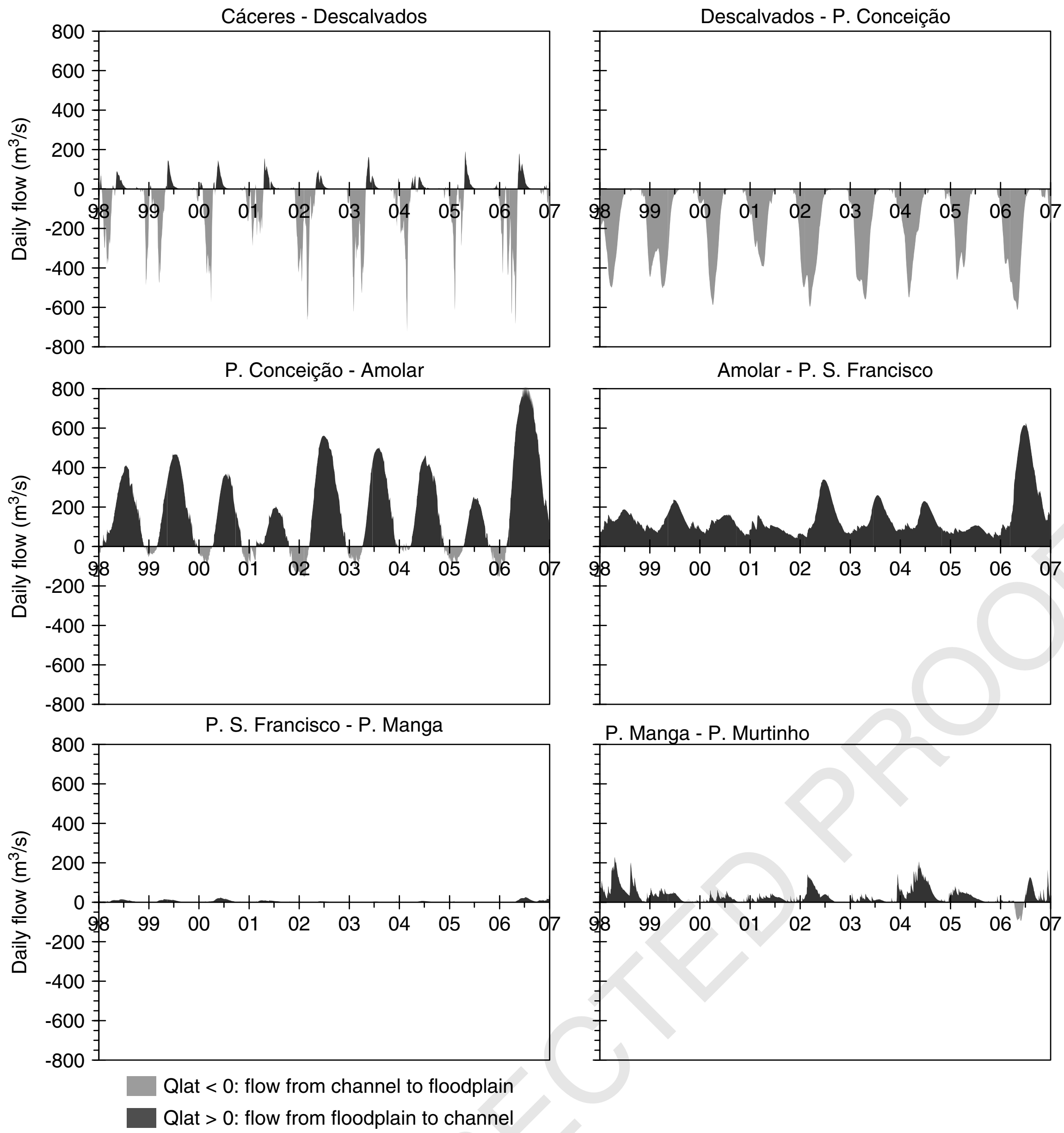

Figure 10. Lateral exchanges of water between main channel and floodplain simulated by SIRIPLAN along the modelled reach of Paraguay River, separated into six river reaches between each, two consecutive gauging stations: Cáceres, Descalvados, P. Conceição, Amolar, P. S. Francisco, P. Manga and P. Murtinho

at Descalvados, 12% at P. Conceição, 11% at Amolar, 13% at P. S. Francisco, 9% at P. Manga and 13% at P. Murtinho. In terms of volume error, the results obtained ranged from −6·1% at P. Murtinho to 7·6% at P. Conceição station. Manning coefficients ranged from 0·012 to 0·055.

Hydrographs along Paraguay River have marked seasonality, as can be seen on Figure 8d (P. Conceição station), Figure 8e (Amolar) and Figure 8f (P. Manga), which were quite well reproduced by the developed model, despite some discrepancies between observed and estimated hydrographs, as the overestimation of recession flows and underestimation of peak flows in some years.

It is important to highlight the model ability for differentiating the intensity of the seasonal flood among years. For instance, at P. Manga station, which has a drainage area greater than 330 000 km^2, the SIRIPLAN was able to estimate the reduced peak flows (less than 1800 m^3/s) of the floods of the years 2001 and 2005 and the large flood of 2002 (peak flow around 2700 m^3/s).

The simulated lateral flow in the Paraguay River reach from P. S. Francisco to P. Manga (almost 200 km length) was negligible, while a loss of water from main channel to floodplain achieving peak flows up to 600 m^3/s was estimated for the reach between Descalvados and P. Conceição (∼120 km). Along the 21-km long reach downstream of the confluence of Cuiabá River up to Amolar station, a gain of water from floodplain to main channel was simulated. This gain occurred throughout the entire year, with peak flows up to 330 m^3/s in the period June–July and flows up to 30 m^3/s in the other months.

To better analyse the channel–floodplain water exchanges along the modelled reach of the Paraguay River, the estimates of lateral flows for each reach delimited by two consecutive streamflow gauging stations is shown in Figure 10. This figure shows distinct patterns of lateral water exchanges along the upper, middle and lower reaches of the Paraguay River. A loss of water from channel to floodplain prevails in the most upper part of the Paraguay River, from Cáceres (boundary condition) to Descalvados station. Simulated lateral flows from channel to floodplain achieved peaks of up to 650 m^3/s in the reach between Cáceres and Descalvados, and up to 590 m^3/s in the reach between Descalvados and P. Conceição. In the reach Cáceres–Descalvados, results show that water flows from channel to floodplain mostly during the period December–April and in the opposite direction during the period May–July, with null flows from August to November. In the downstream reach (Descalvados–P.Conceição), null lateral flows were simulated from July to November, with a loss of water from channel to floodplain over the rest of the year.

In the middle part of the Paraguay River, downstream of P. Conceição station and upstream of P. S. Francisco, the simulated lateral exchanges of water were predominantly a gain from floodplains to main channel. Indeed, the model simulated that this reach of the Paraguay River receives contribution propagated from its upstream floodplains and also drained by the floodplains of Cuiabá River. The simulated lateral peak flows were up to 800 m^3/s in the reach between P. Conceição and Amolar, and up to 620 m^3/s in the reach between Amolar and P. S. Francisco. In the former reach, lateral water loss from channel to floodplain was simulated in the period December–March, with flows in the opposite direction during the following months. In the latter reach, a gain of water from floodplain to channel was simulated as occurring over the entire year.

For the lower part of the Paraguay River, from P. S. Francisco to P. Murtinho station, simulated lateral flows were relatively small, in comparison to the flows of the upstream reaches. Along the reach between P. S. Francisco and P. Manga, these flows were approximately null, while a gain of water less than 200 m^3/s was simulated along the reach between P. Manga and P. Murtinho stations.

Floodplain inundation

Typical inundation maps of a dry and wet period are shown in Figure 11, relative to the dates 6 October 2004 and 13 February 2005, respectively. The estimates of inundation extent produced by Padovani (2007) for these same dates are also shown in this figure. The correspondent measures of fit between simulated (our results) and estimated (Padovani's results) inundation maps are given in Table IV.

The model was capable to reproduce part of the major permanent inundated areas during the dry period, which are exclusively due to water spilling from main channels and flowing along floodplain. These areas are located along the north and central portions of Paraguay River, in the reach between Descalvados and P. Manga gauging stations, along the floodplains of the lower reach of Cuiabá River and along both margins of the Taquari River. Also, the inundation along Taquari floodplains is consistent with the expected pattern, as this region comprises the distributary fan lobe of the Taquari alluvial megafan (Assine, 2005). However, considering the estimates of Padovani (2007) as correct, these major flooded

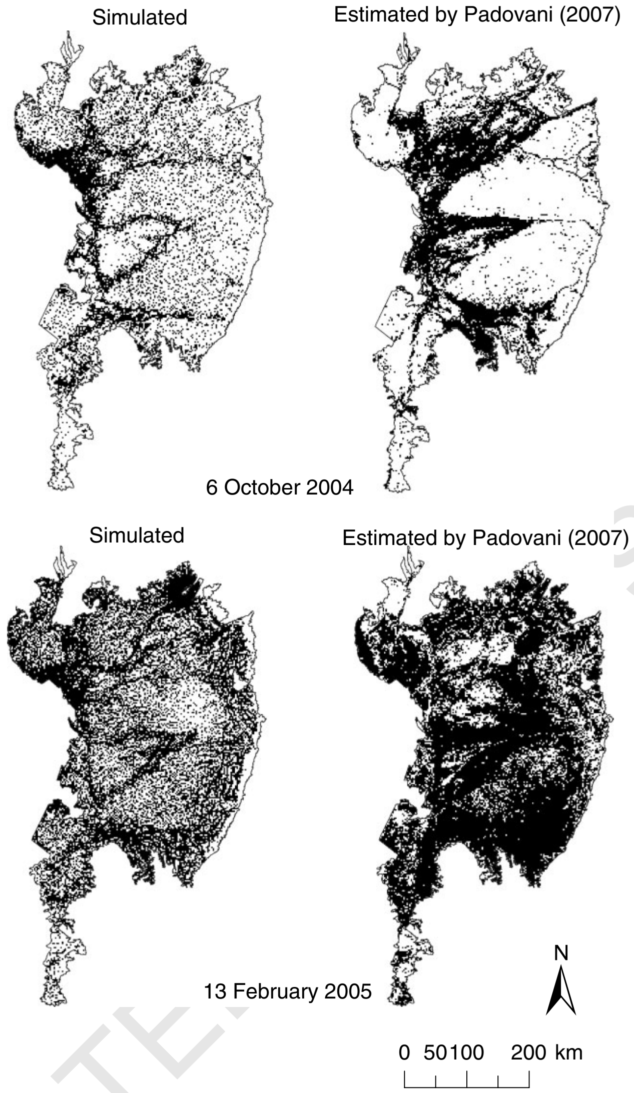

Figure 11. Inundation maps of Pantanal simulated and estimated by Padovani (2007), for two dates: 6 October 2004 (dry period) and 13 February 2005 (wet period)

Table IV. Skill scores of the comparison between inundation maps estimated by Padovani (2007) and simulated with SIRIPLAN, at two dates

Accuracy measure	Dry period (6 October 2004)	Wet period (13 February 2005)
PC	0·60	0·57
CSI	0·24	0·51
POD	0·37	0·59
FAR	0·60	0·23

areas were underestimated by the model, as is clear by visual comparison of both maps. This underestimation resulted in the low CSI and POD skill scores. About 60% (PC = 0·60) of the pixels were in agreement between these two inundation maps, i.e. 60% of the area was wet or dry simultaneously on both maps. However, disregarding the coincident dry pixels on both maps, the agreement between them reaches 24% (CSI = 0·24). From the area estimated as flooded in Padovani's work, 37% was also flooded in the simulated map (POD = 0·37). On the contrary, the obtained FAR score means that, from the area simulated as flooded, 60% was estimated as dry by Padovani (2007), and this relatively high value is mostly due to dispersed isolated pixels wrongly simulated as flooded by the model. In terms of total area, the model simulated 40 491 km^2 as flooded areas, which corresponds to 29·2% of the Pantanal, while the estimates of Padovani (2007) indicate an inundation extent of 45 135 km^2 (32·6% of total) (Table V).

During floods, the loss of water from main channels to floodplains is increased and the most important flooded areas identified in the dry period become larger and deeper. However, the major difference between inundation maps of dry and wet periods is that in the wet period the flooded areas cover a much larger extension along the whole domain. Although with prevailing shallow water depths, the simulated flooded area on 13 February 2005 covers almost twice the extent estimated at 6 October 2004, i.e. a flooded area of about 76 406 km^2 or 55·2% of the entire Pantanal. The estimates of Padovani (2007) show an even larger flooded area, of about 100 393 km^2 (72·5% of total), and indicate again an underestimation trend on model results, but weaker than that for the dry period. In terms of skill scores, the general agreement between simulated and estimated inundation maps was increased in comparison to the dry period. Although the PC index was almost equal between the two periods, the CSI and POD indices were quite improved at this time, with CSI = 0·51 and POD = 0·59. Also, the FAR has decreased (FAR = 0·23), meaning that only 23% of the area simulated as flooded was dry in the inundation map of Padovani (2007).

In comparison to others studies of floodplain inundation modelling, our CSI scores are relatively similar with them. For instance, the greater difficulty to reproduce the inundation extent during the dry period is also pointed out by Wilson *et al.* (2007), which was the unique previous study •we found that assessed inundation map during dry period. Those authors used the LISFLOOD-FP model to simulate part of the Amazon River and Purus tributary, obtaining CSI = 0·23, approximately the same score we achieved. They state that their model inability to simulate low water inundation extent is mostly due to not including floodplain vertical hydrological processes and the SRTM DEM aggregation, which makes difficult the representation of complex, small-scale topography controlling part of the floodplain drying out process. Although we have included representation of evapotranspiration and infiltration processes, the simplicity of adopted schemes together with the aggregation of SRTM DEM to the 2 km resolution may have reduced model capability on reproducing the full drainage of the floodplain. The sparse pluviometer network and uncertainties on precipitation estimates may also have contributed to this model inability. For the wet period, our CSI score of 0·51 is similar to the lower limit of the range of results obtained by others authors varying model parameters or structure, such as Wilson *et al.* (2007), Tayefi *et al.* (2007), Horritt and Bates (2001b) and Bates and De Roo (2000). AQ4

As stated before, during the dry period, the inundation extent was almost limited to the major permanent flooded areas resultant from water spilling from main channel to floodplains. During the wet period, regions not directly connected to overbank flow from main channels were flooded due to delayed drainage of precipitation. This input of water to the floodplain gives origin to local water accumulation which drains slowly, or is evaporated in the following dry period, resulting in a marked seasonal variation in total inundated area as illustrated in Figure 12. Peaks of total inundated areas simulated by the model ranged from 100 000 to 126 000 km^2 along the simulation period, which are similar to the maximum values of inundation estimated by Hamilton *et al.* (1996) for a different period (1979–1987). The total inundated areas during dry periods simulated with SIRIPLAN ranged from 35 000 to 45 000 km^2, while the mentioned study estimated much smaller minimum inundated areas, of up to 11 000 km^2. This result could indicate an overestimation of our inundated area during dry period. However, given that the estimate of inundation extent of Padovani (2007) for the date 6 October 2004 (dry

Table V. Flooded and dry total areas over Pantanal on two dates simulated by SIRIPLAN and estimated by Padovani (2007)

Floodplain	Dry period (6 October 2004)				Wet period (13 February 2005)			
	Simulated		Estimated by Padovani (2007)		Simulated		Estimated by Padovani (2007)	
	Area (km^2)	Percentage of total area	Area (km^2)	Percentage of total area	Area (km^2)	Percentage of total area	Area (km^2)	Percentage of total area
Flooded	40 491	29·2	45 135	32·6	76 406	55·2	100 393	72·5
Dry	97 946	70·8	93 302	67·4	62 032	44·8	38 044	27·5
Total	138 437	100·0	138 437	100·0	138 437	100·0	138 437	100·0

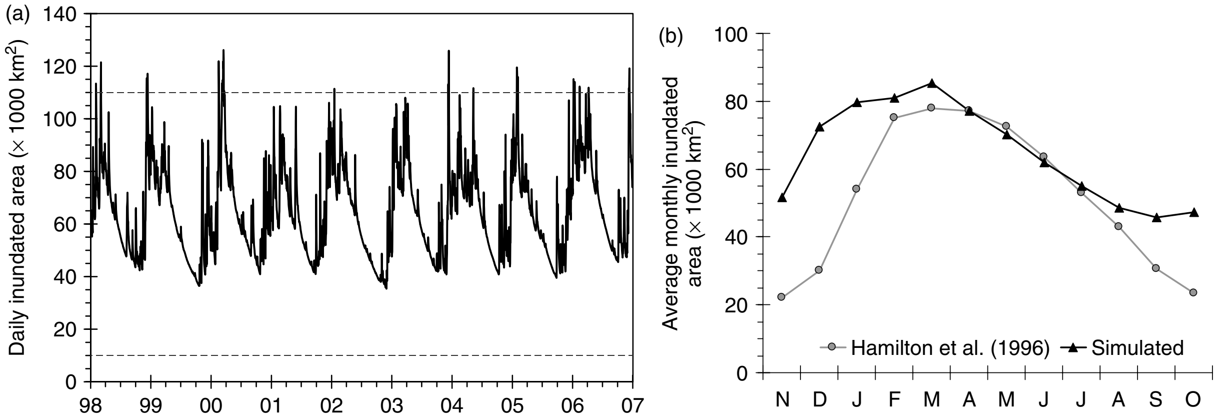

Figure 12. (a) Daily inundated areas simulated over Pantanal [the horizontal grey lines represent the maximum and minimum values estimated by Hamilton *et al*. (1996) for the period 1979–1987] and (b) average monthly inundated areas simulated along the period from 1 January 1998 to 31 December 2006 and estimated by Hamilton *et al*. (1996) for the period 1979–1987

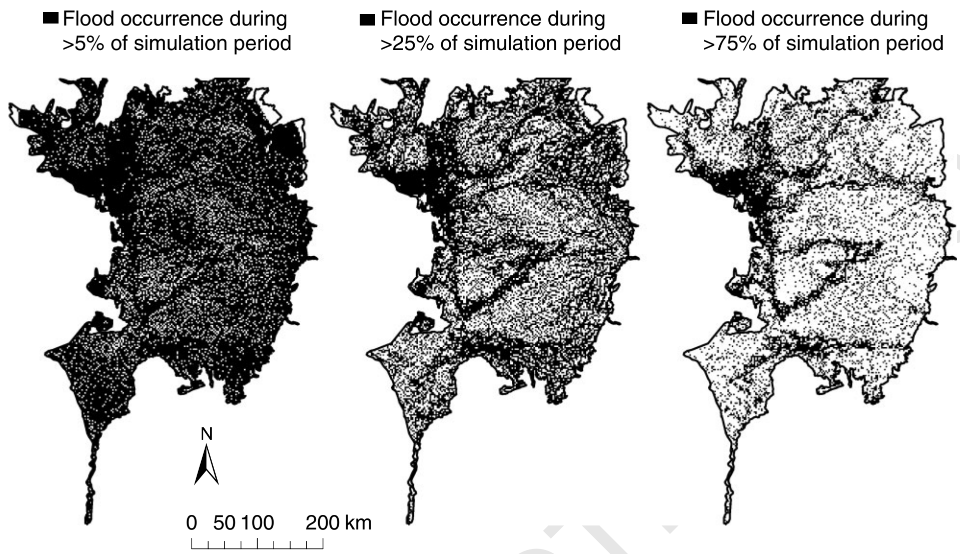

Figure 13. Maps showing areas subject to inundation during frequencies greater than 5%, 25% or 75% of simulation period

period) corresponds to an area of about 45 000 km^2 and seems consistent to expected inundation patterns of Pantanal, may be the results of Hamilton *et al*. (1996) are underestimated or their period of analysis was much more drier than our area.

Comparison of average monthly estimates shows that in our study the peak of flooding occurred between 1 and 2 months in advance relative to the results of Hamilton *et al*. (1996) (Figure 9b). Again, it can be noted the difference on inundated areas in the dry period between the two studies. Nevertheless, it is worth noting the importance of including the vertical water balance on floodplain modelling and the capability of SIRIPLAN to simulate the Pantanal seasonal flood pulse.

The model capability to simulate the major permanent flooded areas are also highlighted by maps shown in Figure 13, which provides an analysis of simulated inundation frequency spatially distributed over Pantanal. The maps in this figure show the areas that were inundated during time periods greater than 5%, 25% and 75% of the simulation period (considering the 9 years from 1 January 1998 to 31 December 2006). These inundation frequencies were calculated regardless of being during consecutive days or not. Approximately 32% (43 624 km^2) of the Pantanal was flooded during more than 75% of the simulation period, while 58% (80 330 km^2) of Pantanal was flooded during more than 25% of the simulation period. This area increases to 115 033 km^2 (83% of total) when the 5% frequency threshold is considered, and it goes to the limit of 100% of Pantanal area as the threshold approaches zero, i.e. the entire Pantanal was flooded in at least 1 day of the simulation period. On the contrary, when the frequency threshold approaches 100%, i.e. considering solely pixels which were strictly permanently inundated, the area covers roughly 22% of entire Pantanal (~30 000 km^2).

SUMMARY AND CONCLUSIONS

This paper presents the hydrologic simulation system SIRIPLAN, developed for simulating the flow regime and spatial inundation over large-scale networks of rivers and floodplains. The SIRIPLAN couples the 1D hydrodynamic model IPH4 for simulating main channel flow to a 2D raster-based floodplain model, which simulates the floodplain inundation dynamics. Auxiliary modules simulate the vertical water processes of precipitation, infiltration and evapotranspiration over floodplains and water exchanges between channels and floodplains.

The application example of the SIRIPLAN to the UPRB, which includes the Pantanal, one of the largest wetlands of the world, showed the viability and adequacy of the proposed approach. A total of 3965 km of main channels and 140 000 km^2 of floodplains were simulated for a time period of 11 years. The computational routines developed for establishing the topological connections between channel and floodplain discretization elements strongly reduced the effort and time needed on input data preparation. Additionally, the use of a parallelization scheme through OpenMP method for two loops of the floodplain model has proven to be a satisfactory way to reduce run time, which may allow higher level of floodplain spatial discretization.

The model was capable to reproduce the flow regime along main channels of Paraguay River and its tributaries. Distinct cases were satisfactorily simulated, such as rivers that present enormous loss of water from main channel to floodplain during the floods, rivers where this loss occurs during both the flood and dry periods, rivers where there is a gain of water from floodplains to main channel and rivers which do not exchange water laterally. For instance, it must be emphasized that the ability of the proposed model to simulate the complex behaviour of channel–floodplain interactions specifically in the region of the S. Lourenço and Piquiri Rivers, in which the water spills over the channel of the S. Lourenço River, inundates the floodplain and propagates over it until reaching and contributing to the flow of the main channel of the Piquiri River.

The SIRIPLAN was also able to reproduce the Pantanal seasonal flood pulse, with estimates of inundated area varying from 35 000 to 45 000 km^2 in the dry period and ranging from 100 000 to 126 000 km^2 in the wet period. These estimates were consistent with the results obtained by a earlier study, which was based on coarse-resolution satellite images and analysed a distinct period of time, but with greater inundation area during the dry period.

Floodplain inundation maps obtained with SIRIPLAN were consistent with previous knowledge of Pantanal dynamics, presenting regions permanently inundated, as well as regions seasonally inundated due to precipitation and overbank flow of rivers. However, comparison to inundation maps estimated by a previous satellite-based study indicates that permanently flooded areas may have been underestimated. Performance measures derived from this comparison were similar to part of those reported in literature. Given that our study domain is several times larger than of those studies, and the complexity involved in contrast to scarce data availability, we can consider we achieved reasonable results.

Furthermore, this paper presented the first results of our effort for mathematic modelling floodplain dynamics over Pantanal, using the proposed SIRIPLAN simulation system. Despite consistent and promising results, further work is necessary, mostly for analysing the sensitivity of the inundation model to floodplain parameters, time step and uncertainty of precipitation estimates and improving representation of infiltration and evapotranspiration processes over floodplains.

ACKNOWLEDGEMENTS

The first author was supported by Conselho Nacional de Desenvolvimento Científico e Tecnológico (CNPq).

REFERENCES

Abbott MB. 1979. *Computational Hydraulics—Elements of the Theory of Free Surface Flows*, Pitman Advanced Publishing Program: London; 326.

Assine ML. 2005. River avulsions on the Taquari megafan, Pantanal wetland, Brazil. *Geomorphology* **70**: 357–371. DOI: 10.1016/j.geomorph.2005.02.013.

Bates PD. 2004. Remote sensing and flood inundation modelling. *Hydrological Processes* **18**: 2593–2597. DOI: 10.1002/hyp.5649.

Bates PD, De Roo AP. 2000. A simple raster-based model for flood inundation simulation. *Journal of Hydrology* **236**: 54–77. DOI: 10.1016/S0022-1694(00)00278-X.

Bates PD, Dawson RJ, Hall JW, Horritt MS, Nicholls RJ, Wicks J, Hassan MA. 2005. Simplified two-dimensional numerical modelling of coastal flooding and example applications. *Coastal Engineering* **52**: 793–810. DOI: 10.1016/j.coastaleng.2005.06.001.

Bates PD, Wilson MD, Horritt MS, Mason DC, Holden N, Currie A. 2006. Reach scale floodplain inundation dynamics observed using airborne synthetic aperture radar imagery: data analysis and modelling. *Journal of Hydrology* **328**(1–2): 306–318. DOI: 10.1016/j.jhydrol.2005.12.028.

Beven K, Freer J. 2001. Equifinality, data assimilation, and uncertainty estimation in mechanistic modelling of complex environmental systems using the GLUE methodology. *Journal of Hydrology* **249**(1–4): 11–29. DOI: 10.1016/S0022-1694(01)00421-8.

Biancamaria S, Bates PD, Boone A, Mognard NM. 2009. Large-scale coupled hydrologic and hydraulic modelling of the Ob river in Siberia. *Journal of Hydrology* **379**: 136–150. DOI: 10.1016/j.jhydrol.2009.09.054.

Bordas MP. 1996. The Pantanal: an ecosystem in need of protection. *International Journal of Sediment Research* **11**(3): 34–39.

Bradbrook KF, Lane SN, Waller SG, Bates PD. 2004. Two dimensional diffusion wave modelling on flood inundation using a simplified channel representation. *International Journal of River Basin Management* **2**(3): 211–223.

Brasil Ministério do Meio Ambiente dos Recursos Hídricos e da Amazônia Legal. 1997. *Plano de Conservação da Bacia do Alto Paraguai (Pantanal)—PCBAP: Análise Integrada e Prognóstico da Bacia do Alto Paraguai*, MMA/PNMA: Brasília (Brazil); 369.

Burrough PA, McDonnel RA. 1998. *Principles of Geographical Information Systems: Spatial Information Systems and Geostatistics*, Oxford University Press: Oxford; 333.

Chapman B, Jost G, Van Der Paas AR. 2008. *Using OpenMP—Portable Shared Memory Parallel Programming*, The MIT Press: Massachusetts; 378.

Chatterjee C, Fröster S, Bronstert A. 2008. Comparison of hydrodynamic models of different complexities to model floods with emergency storage areas. *Hydrological Processes* **22**(24): 4695–4709. DOI: 10.1002/hyp.7079.

Chow VT. 1959. *Open-channel Hydraulics*, McGraw-Hill: New York; 680.

Chow VT. 1964. *Handbook of Applied Hydrology. A Compendium of Water-resources Technology*, McGraw-Hill: New York; 7–25.

Collischonn W, Allasia D, Silva BC, Tucci CEM. 2007. The MGB-IPH model for large scale rainfall runoff modelling. *Hydrological Sciences Journal* **52**(5): 878–895. DOI: 10.1623/hysj.52.5.878.

Cunge JA, Holly FM, Verwey A. 1981. *Practical Aspects of Computational River Hydraulics*, Pitman Publishing: Boston; 420.

Da Silva CJ, Girard P. 2004. New challenges in the management of the Brazilian Pantanal and catchment area. *Wetlands Ecology and Management* **12**: 553–561. DOI: 10.1007/s11273-005-1755-0.

DNOS Departamento Nacional de Obras contra as Secas. 1974. *Estudos Hidrológicos da Bacia do Alto Paraguai*, Relatório Técnico UNESCO/PNUD: Rio de Janeiro; 284.

Fairfield J, Leymarie P. 1991. Drainage networks from grid digital elevation models. *Water Resources Research* **27**(5): 709–717.

Fekete BM, Vörösmarty CJ, Lammers RB. 2001. Scaling gridded river networks for macroscale hydrology: development, analysis, and control of error. *Water Resources Research* **37**(7): 1955–1967. DOI: 10.1029/2001WR900024.

AQ5 •Fread DL. 1992. Flow routing. In *Handbook of Hydrology*, Maidment DR (ed). McGraw-Hill.

Gillan P, Jempson M, Rogencamp G. 2005. *The Importance of Combined 2D/1D Modelling of Complex Floodplain—Tatura Case Study*, Fourth Victorian Flood Management Conference: Victoria (Australia).

Hamilton SK. 1999. Potential effects of a major navigation project (Paraguay-Paraná Hidrovía) on inundation in the Pantanal floodplains. *Regulated Rivers: Research and Management* **15**: 289–299.

Hamilton SK, Sippel SJ, Melack JM. 1996. Inundation patterns in the Pantanal wetland of South America determined from passive microwave remote sensing. *Archive Für Hydrobiologie* **137**(1): 1–23.

Hamilton SK, Sippel SJ, Melack JM. 2002. Comparison of inundation patterns among major South American floodplains. *Journal of Geophysical Research* **107**(D20): 8038. DOI: 10.1029/2000JD000306.

Harris MB, Tomas W, Mourão G, Da Silva CJ, Guimarães E, Sonoda F, Fachim E. 2005. Safeguarding the Pantanal wetlands: threats and conservation initiatives. *Conservation Biology* **19**(3): 714–720. DOI: 10.1111/j.1523–1739.2005.00708.x.

Hermanns M. 2002. *Parallel Programming in Fortran 95 Using OpenMP*, Universidad de Madrid: Madrid; 75.

Horritt MS, Bates PD. 2001a. Predicting floodplain inundation: raster-based modelling versus the finite-element approach. *Hydrological Processes* **15**: 825–842. DOI: 10.1111/j.1523–1739.2005.00708.x.

Horritt MS, Bates PD. 2001b. Effects of spatial resolution on a raster based model of flood flow. *Journal of Hydrology* **253**: 239–249. DOI: 10.1016/S0022-1694(01)00490-5.

Hunter NM, Bates PD, Horritt MS, Wilson MD. 2007. Simple spatially-distributed models for predicting flood inundation: a review. *Geomorphology* **90**: 208–225. DOI: 10.1016/j.geomorph.2006.10.021.

Jenson SK, Domingue JO. 1988. Extracting topographic structure from digital elevation data for geographic information system analysis. *Photogrammetric Engineering and Remote Sensing* **54**(11): 1593–1600.

Junk WJ, Cunha CN. 2005. Pantanal: a large South American wetland at a crossroads. *Ecological Engineering* **24**: 391–401. DOI: 10.1016/j.ecoleng.2004.11.012.

Junk WJ, Bayley PB, Sparks RE. 1989. The flood pulse concept in river-floodplain-systems. *Canadian Special Publications for Fisheries and Aquatic Sciences* **106**: 110–127.

Junk WJ, Cunha CN, Wantzen KM, Petermann P, Strüssmann C, Marques MI, Adis J. 2006. Biodiversity and its conservation in the Pantanal of Mato Grosso, Brazil. *Aquatic Sciences* **68**(3): 278–309. DOI: 10.1007/s00027-006-0851-4.

Kummerow C, Simpson J, Thiele O, Barnes W, Chang ATC, Stocker E, Adler RF, Hou A, Kakar R, Wentz F, Ashcroft P, Kozu T, Hong Y, Okamoto K, Iguchi T, Kuroiwa H, Im E, Haddad Z, Huffman G, Ferrier B, Olson WS, Zipser E, Smith EA, Wilheit TT, North G, Krishnamurti T, Nakamura K. 2000. The status of the Tropical Rainfall Measuring Mission (TRMM) after two years in orbit. *Journal of Applied Meteorology* **39**: 1965–1982.

Mark DM. 1984. Automated detection of drainage networks from digital elevation models. *Cartographica* **21**(2–3): 168–178.

Neal J, Fewtrell T, Trigg M. 2009. Parallelisation of storage cell flood models using OpenMP. *Environmental Modelling and Software* **24**: 872–877. DOI: 10.1016/j.envsoft.2008.12.004.

Padovani CR. 2007. Monitoramento e sistema de alerta de inundações do Pantanal: proposta e resultados preliminares. In 2° SIBRADEN—Simpósio Brasileiro de Desastres Naturais e Tecnológicos, Santos (Brazil).

Paiva RCD. 2009. Modelagem hidrológica e hidrodinâmica de grandes bacias—estudo de caso: bacia do rio Solimões. MSc dissertation, Instituto de Pesquisas Hidráulicas, Universidade Federal do Rio Grande do Sul, Porto Alegre (Brazil), 182.

Paz AR, Collischonn W, Risso A, Mendes CAB. 2008. Errors in river lengths derived from raster digital elevation models. *Computers and Geosciences* **34**: 1584–1596. DOI: 10.1016/j.cageo.2007.10.009.

Paz AR, Bravo JM, Allasia D, Collischonn W, Tucci CEM. 2010. Large-scale hydrodynamic modelling of a complex river network and floodplains. *Journal of Hydrologic Engineering* **15**(2): 152–165. DOI: 10.1061/(ASCE)HE.1943–5584.0000162.

Pearson D, Horritt MS, Gurney RJ, Mason DC. 2001. The use of remote sensing to validate hydrological models. In *Model Validation—Perspectives in Hydrological Sciences*, Anderson MG, Bates PD (eds). John Wiley and Sons: Chichester; 163–196.

Poff NL, Allan JD, Bain MB, Karr JR, Prestegaard KL, Richter BD, Sparks RE, Stromberg JC. 1997. The natural flow regime: a paradigm for river conservation and restoration. *Bioscience* **47**(11): 769–784.

Postel S, Richter B. 2003. *Rivers for Life: Managing Water for People and Nature*, Island Press: Washington; 253.

Pott A, Pott VJ. 2004. Features and conservation of the Brazilian Pantanal wetland. *Wetlands Ecology and Management* **12**: 547–552. DOI: 10.1007/s11273-005-1754-1.

•Shuttleworth WJ. 1993. Evaporation. In *Handbook of Hydrology*, Maidment DR (ed). McGraw-Hill: New York. AQ6

Tayefi V, Lane SN, Hardy RJ, Yu D. 2007. A comparison of one- and two-dimensional approaches to modelling flood inundation over complex upland floodplains. *Hydrological Processes* **21**(23): 3190–3202. DOI: 10.1002/hyp.6523.

Trigg MA, Wilson MD, Bates PD, Horritt MS, Alsdorf DE, Forsberg BR, Vega MC. 2009. Amazon flood wave hydraulics. *Journal of Hydrology* **374**: 92–105. DOI: 10.1016/j.jhydrol.2009.06.004.

Tucci CEM. 1978. Hydraulic and water quality model for a river network. PhD thesis, Colorado State University, Fort Collins, 218.

Tucci CEM, Clarke RT. 1998. Environmental issues in the la Plata basin. *Water Resources Development* **4**(2): 157–173.

Tucci CEM, Genz F, Clarke RT. 1999. Hydrology of the upper Paraguay basin. In *Management of Latin American River Basins: Amazon, Plata and São Francisco*, Biswas K, Cordeiro N, Braga B, Tortajada C (eds). United Nations University Press: Tokyo.

Tucci CEM, Villanueva A, Collischonn W, Allasia DG, Bravo J, Collischonn B. 2005. *Projeto de Implementação de Práticas de Gerenciamento Integrado de Bacia Hidrográfica para o Pantanal e Bacia do Alto Paraguai, Subprojeto 5·4—Modelo Integrado de Gerenciamento Hidrológico da Bacia do Alto Paraguai*, ANA/GEF/PNUMA/OEA: Porto Alegre (Brazil); 554.

Verwey A. 2001. Latest developments in floodplain modelling—1D/2D integration. *Proceedings of the Conference on Hydraulics in Civil Engineering*, The Institution of Engineers: Australia.

Werner MG, Hunter NM, Bates PD. 2005. Identifiability of distributed floodplain roughness values in flood extent estimation. *Journal of Hydrology* **314**: 139–157. DOI: 10.1016/j.jhydrol.2005.03.012.

Wigmosta MS, Vail LW, Lettenmaier DP. 1994. A distributed hydrology-vegetation model for complex terrain. *Water Resources Research* **30**(6): 1665–1679.

•Wilks DS. 2006. *Statistical Methods in the Atmospheric Sciences*, 2nd edn, Academic Press: 467 p. AQ7

Wilson M, Bates P, Alsdorf D, Forsberg B, Horritt M. 2007. Modelling large-scale inundation of Amazonian seasonally flooded wetlands. *Geophysical Research Letters* **34**: L15404. DOI: 10.1029/2007GL030156.

QUERIES TO BE ANSWERED BY AUTHOR

IMPORTANT NOTE: Please mark your corrections and answers to these queries directly onto the proof at the relevant place. Do NOT mark your corrections on this query sheet.

Queries from the Copyeditor:

AQ1 Based on the data provided in Figure 6 we have inserted "Upstream of Apa River" for j. Please confirm if this is fine. Also, please provide the percentage of simulation period for j.

AQ2 We have inserted the citation for Table I. Please confirm if the placement is correct.

AQ3 The sentence "Another question concerns… floodplain models" is incomplete. Please provide the missing text.

AQ4 The meaning of the sentence 'which was the unique previous….during dry period' is not clear. Please rephrase for clarity.

AQ5 Please provide place of publication and page range for reference Fread (1992).

AQ6 Please provide page range for references Shuttleworth (1993) and Tucci, *et al*. (1999).

AQ7 Please provide the place of publication for reference Wilks (2006).

Required Software to eAnnotate PDFs: Adobe Acrobat Professional or Acrobat Reader (version 8.0 or above).
The Latest version of Acrobat Reader is free: http://www.adobe.com/products/acrobat/readstep2.html

Once you have Acrobat Reader 8, or higher, open on your PC you should see the Commenting Toolbar:

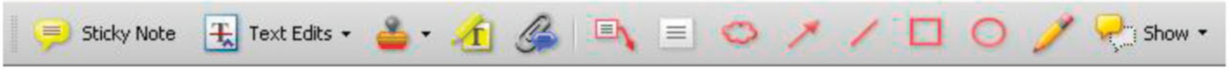

****(If the above toolbar does not appear automatically go to *Tools>Comment & Markup>Show Comment & Markup Toolbar*)****

1. Replacement Text Tool — For replacing text.

Strikes a line through text and opens up a replacement text box.

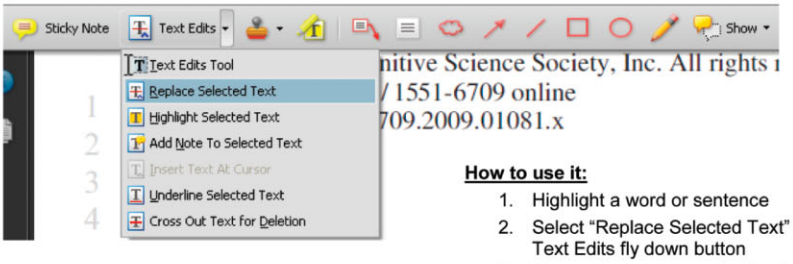

How to use it:

1. Highlight a word or sentence
2. Select "Replace Selected Text" from the Text Edits fly down button
3. Type replacement text in blue box

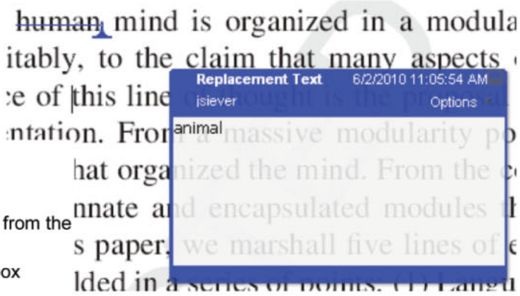

2. Cross-out Text Tool — For deleting text.

Strikes a red line through selected text.

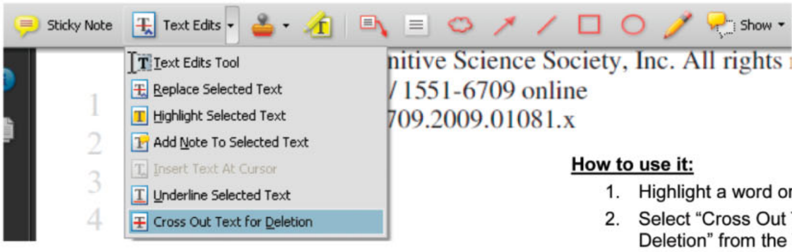

How to use it:

1. Highlight a word or sentence
2. Select "Cross Out Text for Deletion" from the Text Edits fly down button

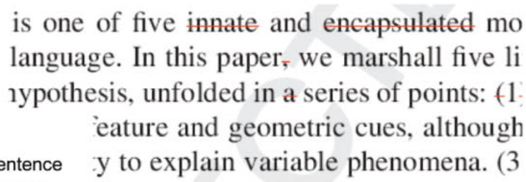

3. Highlight Tool — For highlighting a selection to be changed to bold or italic.

Highlights text in yellow and opens up a text box.

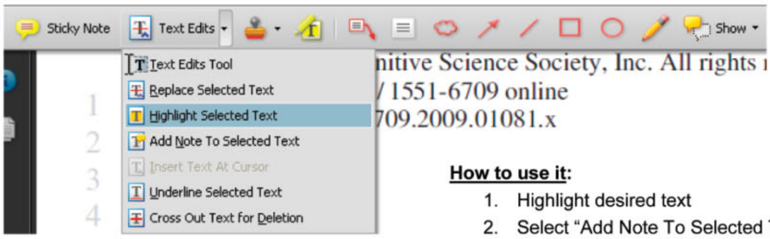

How to use it:

1. Highlight desired text
2. Select "Add Note To Selected Text" from the Text Edits fly down button
3. Type a note detailing required change in the yellow box

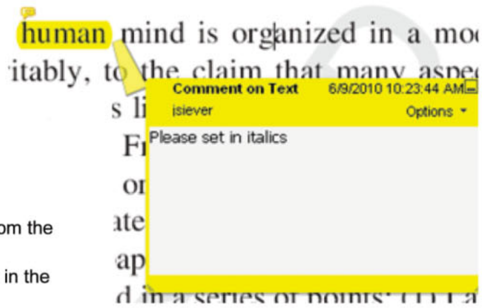

4. Note Tool — For making notes at specific points in the text

Marks a point on the paper where a note or question needs to be addressed.

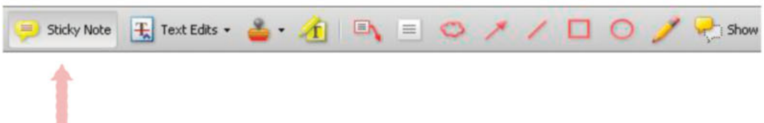

How to use it:

1. Select the Sticky Note icon from the commenting toolbar
2. Click where the yellow speech bubble symbol needs to appear and a yellow text box will appear
3. Type comment into the yellow text box

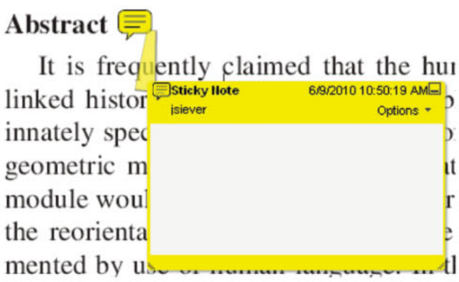

5. Drawing Markup Tools — For circling parts of figures or spaces that require changes

These tools allow you to draw circles, lines and comment on these marks.

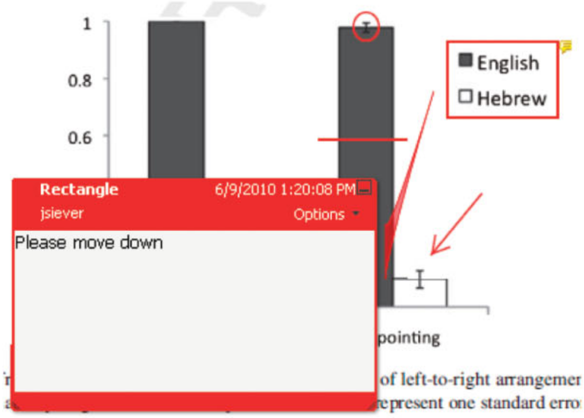

How to use it:

1. Click on one of shape icons in the Commenting Toolbar
2. Draw the selected shape with the cursor
3. Once finished, move the cursor over the shape until an arrowhead appears and double click
4. Type the details of the required change in the red box

6. Attach File Tool — For inserting large amounts of text or replacement figures as a files.

Inserts symbol and speech bubble where a file has been inserted.

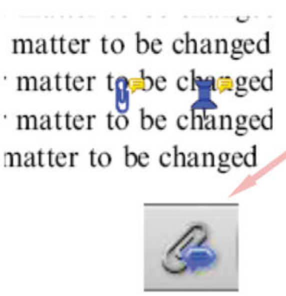

How to use it:

1. Right click on the Commenting Toolbar
2. Select "Attach a File as a Comment"
3. Click on paperclip icon that appears in the Commenting Toolbar
4. Click where you want to insert the attachment
5. Select the saved file from your PC or network
6. Select type of icon to appear (paperclip, graph, attachment or tag) and close

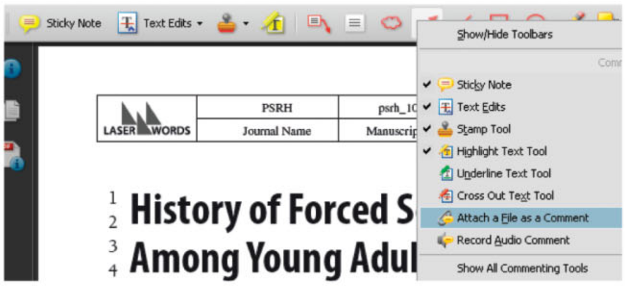

7. Approved Tool (Stamp) — For approving a proof if no corrections are required.

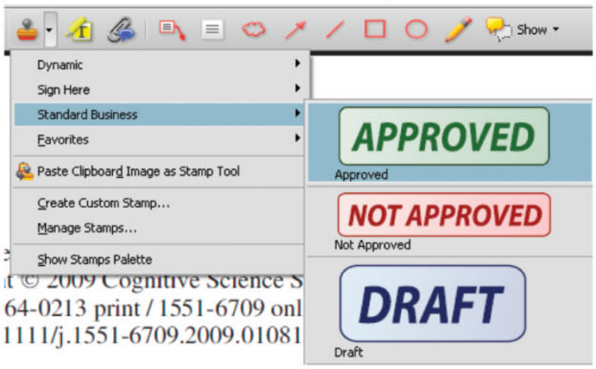

How to use it:

1. Click on the Stamp Tool in the toolbar
2. Select the Approved rubber stamp from the 'standard business' selection
3. Click on the text where you want to rubber stamp to appear (usually first page)

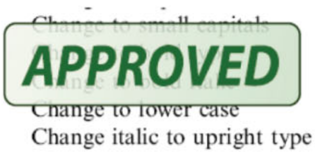

Help

For further information on how to annotate proofs click on the Help button to activate a list of instructions:

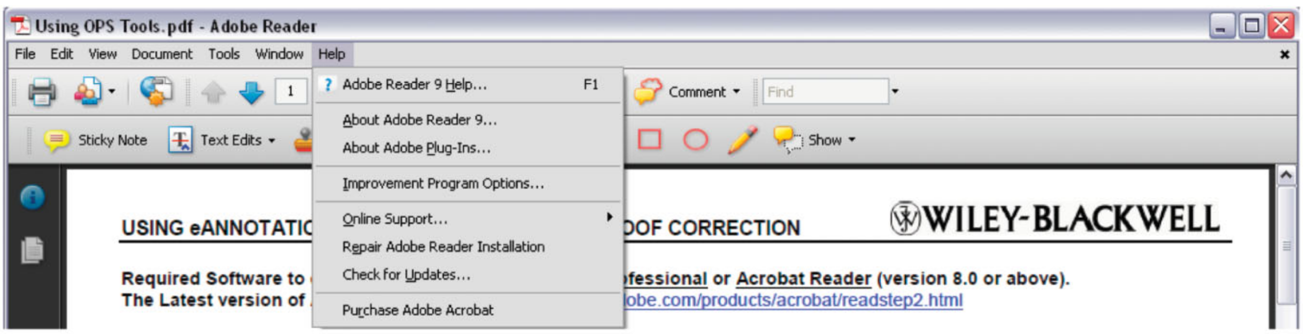

WILEY AUTHOR DISCOUNT CLUB

We would like to show our appreciation to you, a highly valued contributor to Wiley's publications, by offering a **unique 25% discount** off the published price of any of our books*.

All you need to do is apply for the **Wiley Author Discount Card** by completing the attached form and returning it to us at the following address:

The Database Group (Author Club)
John Wiley & Sons Ltd
The Atrium
Southern Gate
Chichester
PO19 8SQ
UK

Alternatively, you can **register online** at www.wileyeurope.com/go/authordiscount
Please pass on details of this offer to any co-authors or fellow contributors.

After registering you will receive your Wiley Author Discount Card with a special promotion code, which you will need to quote whenever you order books direct from us.

The quickest way to order your books from us is via our European website at:

http://www.wileyeurope.com

Key benefits to using the site and ordering online include:

- Real-time SECURE on-line ordering
- Easy catalogue browsing
- Dedicated Author resource centre
- Opportunity to sign up for subject-orientated e-mail alerts

Alternatively, you can order direct through Customer Services at:
cs-books@wiley.co.uk, or call +44 (0)1243 843294, fax +44 (0)1243 843303

So take advantage of this great offer and return your completed form today.

Yours sincerely,

Verity Leaver
Group Marketing Manager
author@wiley.co.uk

*TERMS AND CONDITIONS
This offer is exclusive to Wiley Authors, Editors, Contributors and Editorial Board Members in acquiring books for their personal use. There must be no resale through any channel. The offer is subject to stock availability and cannot be applied retrospectively. This entitlement cannot be used in conjunction with any other special offer. Wiley reserves the right to amend the terms of the offer at any time.

WILEY

REGISTRATION FORM
For Wiley Author Club Discount Card

To enjoy your 25% discount, tell us your areas of interest and you will receive relevant catalogues or leaflets from which to select your books. Please indicate your specific subject areas below.

Accounting [ ]
- Public [ ]
- Corporate [ ]

Chemistry [ ]
- Analytical [ ]
- Industrial/Safety [ ]
- Organic [ ]
- Inorganic [ ]
- Polymer [ ]
- Spectroscopy [ ]

Encyclopedia/Reference [ ]
- Business/Finance [ ]
- Life Sciences [ ]
- Medical Sciences [ ]
- Physical Sciences [ ]
- Technology [ ]

Earth & Environmental Science [ ]

Hospitality [ ]

Genetics [ ]
- Bioinformatics/ Computational Biology [ ]
- Proteomics [ ]
- Genomics [ ]
- Gene Mapping [ ]
- Clinical Genetics [ ]

Medical Science [ ]
- Cardiovascular [ ]
- Diabetes [ ]
- Endocrinology [ ]
- Imaging [ ]
- Obstetrics/Gynaecology [ ]
- Oncology [ ]
- Pharmacology [ ]
- Psychiatry [ ]

Non-Profit [ ]

Architecture [ ]

Business/Management [ ]

Computer Science [ ]
- Database/Data Warehouse [ ]
- Internet Business [ ]
- Networking [ ]
- Programming/Software Development [ ]
- Object Technology [ ]

Engineering [ ]
- Civil [ ]
- Communications Technology [ ]
- Electronic [ ]
- Environmental [ ]
- Industrial [ ]
- Mechanical [ ]

Finance/Investing [ ]
- Economics [ ]
- Institutional [ ]
- Personal Finance [ ]

Life Science [ ]

Landscape Architecture [ ]

Mathematics [ ]
Statistics [ ]

Manufacturing [ ]

Materials Science [ ]

Psychology [ ]
- Clinical [ ]
- Forensic [ ]
- Social & Personality [ ]
- Health & Sport [ ]
- Cognitive [ ]
- Organizational [ ]
- Developmental & Special Ed [ ]
- Child Welfare [ ]
- Self-Help [ ]

Physics/Physical Science [ ]

Please complete the next page /

I confirm that I am (*delete where not applicable):

a **Wiley** Book Author/Editor/Contributor* of the following book(s):
ISBN:
ISBN:

a **Wiley** Journal Editor/Contributor/Editorial Board Member* of the following journal(s):

SIGNATURE: .... Date: ....

PLEASE COMPLETE THE FOLLOWING DETAILS IN BLOCK CAPITALS:

TITLE: (e.g. Mr, Mrs, Dr) .... FULL NAME: ....

JOB TITLE (or Occupation): ....

DEPARTMENT: ....

COMPANY/INSTITUTION: ....

ADDRESS: ....

....

TOWN/CITY: ....

COUNTY/STATE: ....

COUNTRY: ....

POSTCODE/ZIP CODE: ....

DAYTIME TEL: ....

FAX: ....

E-MAIL: ....

YOUR PERSONAL DATA
We, John Wiley & Sons Ltd, will use the information you have provided to fulfil your request. In addition, we would like to:

1. Use your information to keep you informed by post of titles and offers of interest to you and available from us or other Wiley Group companies worldwide, and may supply your details to members of the Wiley Group for this purpose.
   [ ] Please tick the box if you do **NOT** wish to receive this information

2. Share your information with other carefully selected companies so that they may contact you by post with details of titles and offers that may be of interest to you.
   [ ] Please tick the box if you do **NOT** wish to receive this information.

E-MAIL ALERTING SERVICE
We also offer an alerting service to our author base via e-mail, with regular special offers and competitions. If you **DO** wish to receive these, please opt in by ticking the box [ ].

If, at any time, you wish to stop receiving information, please contact the Database Group (databasegroup@wiley.co.uk) at John Wiley & Sons Ltd, The Atrium, Southern Gate, Chichester, PO19 8SQ, UK.

TERMS & CONDITIONS
This offer is exclusive to Wiley Authors, Editors, Contributors and Editorial Board Members in acquiring books for their personal use. There should be no resale through any channel. The offer is subject to stock availability and may not be applied retrospectively. This entitlement cannot be used in conjunction with any other special offer. Wiley reserves the right to vary the terms of the offer at any time.

PLEASE RETURN THIS FORM TO:
Database Group (Author Club), John Wiley & Sons Ltd, The Atrium, Southern Gate, Chichester, PO19 8SQ, UK author@wiley.co.uk
Fax: +44 (0)1243 770154